Applied Energy 298 (2021) 117159

Contents lists available at ScienceDirect

Applied Energy

journal homepage: www.elsevier.com/locate/apenergy

An integrated smart home energy management model based on a pyramid taxonomy for residential houses with photovoltaic-battery systems

Zhuang Zheng [a,b], Zhankun Sun [c], Jia Pan [d], Xiaowei Luo [a,b,*]

[a] Dept. of Architecture and Civil Engineering, City Univ. of Hong Kong, Hong Kong
[b] Architecture and Civil Engineering Research Center, Shenzhen Research Institute of City University of Hong Kong, Shenzhen, China
[c] Dept. of Management Sciences, City Univ. of Hong Kong, Hong Kong
[d] Department of Computer Science, The University of Hong Kong, Pokfulam, Hong Kong

HIGHLIGHTS

- A general pyramid taxonomy for integrated designs and operations of SHEM.
- An integrated SHEM model for residential houses with PV-battery systems.
- A two-stage stochastic programming model to address uncertain loads/PV generations.
- A distributed asynchronous scheduling and iterative pricing algorithm for PV power-sharing.

ARTICLE INFO

Keywords:
SHEM
Taxonomy
Probabilistic forecasting
User preference inference
Two-stage stochastic programming
Iterative pricing

ABSTRACT

Smart home energy management (SHEM) with residential photovoltaic (PV)-battery systems is a complicated issue with different facets. An integrated SHEM model covering the essential functions is missing. Meanwhile, residential PV-battery systems' optimal operations with renewable energy exchanges and imperfect forecasts are still open challenges. In this study, the research activities in SHEM are firstly organized by a pyramid with four functional layers: (i) Monitoring; (ii) Analyzing and forecasting; (iii) Scheduling; and (iv) Coordinating, which can serve as a standard pathway for developing SHEM. Second, guided by the pyramid taxonomy, an integrated SHEM model is developed for residential houses with PV-battery systems. Assuming a perfect Monitoring layer, we obtain the probabilistic load/PV forecasts and user preference vectors of shiftable appliances based on historical data. Then, we develop a two-stage stochastic programming model for optimal scheduling of single houses with a grid-connected PV-battery system, incorporating the probabilistic forecasts and user preference vectors. A retail electricity market with day-ahead (DA) and real-time (RT) markets is employed for leveraging imperfect forecasts. Finally, we design a distributed coordinating algorithm - Asynchronous Scheduling and Iterative Pricing for PV power-sharing among multiple prosumers based on the single-house scheduling model. Numerical simulations based on realistic loads and PV generation data validated the two-stage stochastic programming model's economic superiority and the distributed PV power-sharing approach compared with the rule-based dispatching and selfish scheduling strategies. We concluded that 1) the modeling of load/PV forecast uncertainties is valuable than averaging or ignoring them, 2) the two-stage stochastic programming model and the DA-RT retail electricity market are beneficial for utilizing imperfect forecasts, and 3) coordinating multiple prosumers could benefit each household by sharing PV and battery investments for revenue or trading with local small prosumers for cost reductions.

1. Introduction

The residential sector shares a significant portion of overall energy and electricity consumption. For example, the residential sector consumed nearly 21% of the total energy consumption in Hong Kong in 2016, and over 70% of these demands were supplied by electricity [1]. From 2006 to 2016, residential buildings' energy and electricity consumption increased with an annual average rate of 1.3% and 2.0%, respectively. It is projected that the proportion of electricity consumption will continue to grow due to the electrification of end-use, such as the penetration of heat pumps and electric vehicles.

* Corresponding author.

https://doi.org/10.1016/j.apenergy.2021.117159
Received 11 February 2021; Received in revised form 12 April 2021; Accepted 23 May 2021

Nomenclature

Abbreviations

A&F	Analyzing & Forecasting
DA/RT	Day-ahead / Real-time
DR	Demand response
EEV	The expectation of the expected value
EVPI	The expected value of perfect information
ILM	Intrusive load monitoring
LOT	Length of operation time
MILP	mixed-integer linear programming
NILM	Non-intrusive load monitoring
PLF	Probabilistic load forecasting
PSF	Pattern sequence forecasting
P2P	Peer-to-peer
PTR	Preferred time range
RP	Recourse problem
SHEM	Smart home energy management
SP	Stochastic programming
SOC	State of charge
TSP	Total selling power
TBP	Total buying power
UTR	Utilization time range
UPV	User preference vector
VSS	Value of the stochastic solution
WS	Wait-and-see

Symbols

i/I	Time slot set I enumerated by index i
j	The iteration index for iterative PV power-sharing algorithm
k/K	Shiftable appliance set K enumerated by index k
$\overline{M}$	A big positive value for disjunct constraints
m/M	The coordinating round M and its index m
n/N	The total number of households N and its index n
s/S	The scenario set S enumerated by index s
ξ	Realizations of uncertain parameters

Parameters

cap^B	The battery installation capacity
cap^{PV}	The PV installation area of the houses
$L_{i,\xi}^{non.}$	The uncertain non-controllable household load
$L^{import\_upper\_lim}$	The upper limit for importing electricity from the RT market
$L^{export\_upper\_lim}$	The upper limit for exporting electricity to the RT market
LOT^k	The length of operation time for k^{th} shiftable appliance
PTR_{lower}^k	Lower bound of the user preferred time range for appliance k
PTR_{upper}^k	Upper bound of the user preferred time range for appliance k
P_k^{rate}	The rated power of k^{th} shiftable appliance
$UPV_{k,i}^{app}$	The user preference value for using appliance k at time slot i
$P_{i,\xi}^{PVunit}$	The PV output of unit panel ($1m^2$) rated at 200 W
$P_{i,\xi}^{PV}$	The PV output with uncertainty parameters ξ realized
p_s	The probability of scenario s
SOC_{min}/SOC_{max}	The lower and upper bounds of the state of charge of the battery
$SOC_{initial}/SOC_{end}$	The initial and final state of charges of the battery
SOC_i	The state of charges of the battery at time slot i
UTR_{lower}^k	Lower bound of the allowed utilization time range of appliance k
UTR_{upper}^k	Upper bound of the allowed utilization time range of appliance k
w_k	The factors weighing the significance of appliance k
$\lambda_i^{buy}/\lambda_i^{sell}$	The buying and selling prices in the DA market
μ_i^{buy}/μ_i^{sell}	The buying and selling prices in the RT market
η	The weighting factor for trading off between electricity bills and user comfort
$\eta_{c/d}$	The battery (dis-)charging efficiency
$\in$	The tolerance value for terminating the iterative PV-sharing algorithm
ρ	The maximum (dis-)charging power of the battery inverter
ΔT	The time interval for programming

Variables

$comfort_i$	The total comfort value for using shiftable appliances at time slot i
$d_{k,i}^{app}/u_{k,i}^{app}$	Two auxiliary binary variables to model 'turn on/off' actions of controllable and non-interruptible appliances
$e_{k,i}^{app}/s_{k,i}^{app}$	Two auxiliary binary variables to calculate the starting and finishing time slots of shiftable appliance k
$E_{i,\xi}$	The battery energy level with uncertainty parameters ξ realized
$h_{i,\xi}$	A binary auxiliary variable for concurrency forbidden constraints
$L_i^{shift.}$	The shiftable household loads
$L_{i,\xi}$	The household load at time slot i with uncertainty parameters ξ realized
$q_{i,\xi}$	A binary auxiliary variable for concurrency forbidden constraints
$start^k/end^k$	The starting and finishing time slots of k^{th} appliance
$u_{i,\xi}^B$	Binary indicator variables of either importing or exporting energy
$x_{k,i}^{app}$	The "ON /OFF" states of k^{th} shiftable appliance at time slot i
$x_i^{import}/x_i^{export}$	The imported and exported electricity from the DA retail market
$y_{i,\xi}^{import}/y_{i,\xi}^{export}$	The imported and exported electricity in the RT market
$y_{i,\xi}^{dis}/y_{i,\xi}^{ch}$	The battery (dis-)charging power in the RT market
$y_{i,s}^{RB}$	The power flows from the PV panel to the battery in the RT market
$y_{i,s}^{RC}$	The power flows from the PV panel to the grid in the RT market
$y_{i,s}^{RL}$	The power flows from PV panel to household load in the RT market
$y_{i,s}^{BL}$	The power flows from battery to household load in the RT market
$y_{i,s}^{BC}$	The power flows from the battery to the grid in the RT market
$y_{i,s}^{CB}$	The power flows from grid to battery in the RT market
$y_{i,s}^{CL}$	The power flows from grid to household load in the RT market
$\alpha_{i,\xi}^{buy}, \alpha_{i,\xi}^{sell}$	The non-negative auxiliary variables for balancing the DA imported electricity with real-time realizations
$\beta_{i,\xi}^{buy}, \beta_{i,\xi}^{sell}$	The non-negative auxiliary variables for balancing the DA exported electricity with the real-time realizations

Research report [2] shows that nearly 15–40% of energy consumption can be reduced by adopting smart home energy management systems (SHEM). Nevertheless, smart home energy (electricity) management is a systematic issue, which needs to combine different functional layers to put it into practice. Zhou et al. [3] presented an overview of the architecture, functional modules, and infrastructures of SHEM. Five functional modules are defined: monitoring, logging, control, management, and alarm. Nevertheless, these modules are not representative as some terms are technical and seldom discussed in the literature (i.e., logging and alarm), or some terms are more inclusive and abstract (i.e., control and management). Yildiz et al. [4] summarized the methods and techniques for using smart meter data and proposed a general guide for comparing different studies in smart metering data applications. Their work justified the necessity for standard-based development, implementation, and evaluation codes of SHEM. There have been many research efforts focusing on various topics of SHEM. For example, the load monitoring concepts and methods in households were reviewed in [5]. The probabilistic load forecasting techniques, methodologies, evaluation methods, and common misunderstandings were studied [6]. Beaudin et al. focused on the different modeling approaches for household devices, uncertainties, objectives, and scheduling strategies and discussed the computational issues associated with the modeling complexities [7]. The neighborhood-level coordination and negotiation techniques for managing demand-side flexibility in residential microgrids were reviewed [8]. However, the relations among different topics were neglected and not thoroughly researched. An integrated study considering all essential components is significant to move SHEM forward and foster practical applications. There is still no single study integrating all the primary functions of SHEM to our best knowledge.

Meanwhile, the residential PV-battery system is becoming economically viable due to technological advances and cost reductions. Recent research shows that solar electricity has achieved grid parity in several countries in both plant-side and user-side, even without government tariff support [9]. According to the annual battery price survey of BloombergNEF [10], the lithium-ion battery pack prices have fallen 89% from above $1100/kWh in 2010 to $137/kWh in 2020. By 2023, the average prices will be close to $100/kWh. Thus, a further and constant increase of distributed PV-battery installation is projected in the near future. The distributed residential PV-battery system could provide many techno-economic benefits, such as solving the mismatch between varying household loads and PV generations and improving solar energies' self-consumption and demand self-sufficiency [11]. However, residential PV-battery systems' operation strategies under uncertain loads and PV generations are still the challenges faced by house owners. The current rule-based dispatch strategy may not exploit the advantages of forecasting information and optimization-based scheduling. Besides, the SHEM with energy transaction capability would be the trend, as the growing number of households are equipped with PV-battery systems. Nevertheless, the proper electricity market for distributed energy systems is still in its infant stage, and many policy issues remain to be solved.

Therefore, we firstly propose a specialized taxonomy for the integrated design and operation of SHEM. We permutate the sub-objectives or technologies in different SHEM developing stages by a pyramid, covering load monitoring, analyzing, forecasting, scheduling and coordinating. By analyzing and clarifying the relationships between the SHEM pyramid's functional layers, one can investigate the prerequisites necessities and the constructive expectations of a single layer to prevent the research efforts' regressive trend and foster the achievable SHEM. Then, guided by the pyramid taxonomy, we design an integrated SHEM model for residential houses with PV-battery systems. Advanced topics, including probabilistic household load/PV forecasting, occupant preference inference, two-stage stochastic scheduling for DA purchase commitment and RT optimal power flows of single households, and power-sharing among multiple prosumers in a community energy market, are integrated into a single model.

The core contributions of this paper are two folds: 1) developing a specialized pyramid taxonomy for standard-based development and implementation of SHEM, which provide an overview of SHEM for novice researchers and general guidance for practitioners; 2) presenting an integrated SHEM model for residential houses with PV-battery systems including essential functions, such as probabilistic forecasting of household loads and PV generations, the user's preference vector modeling for comfort-aware appliance scheduling, two-stage stochastic programming for energy scheduling and distributed coordinating for PV power-sharing among prosumer communities.

2. Literature review

2.1. A taxonomy for smart home energy management

Smart home energy management is a broad research area with different sub-objectives and knowledge domains. To help novice researchers and practitioners quickly obtain an overview of this field and find a standard pathway to practical deployment, a pyramid taxonomy for smart home energy management is designed, as shown in Fig. 1. The taxonomy consists of four primary layers: monitoring, analyzing & forecasting (A&F), scheduling, and coordinating, and their functions and probably involved knowledge domains have also been listed.

The home energy consumption details lay the foundation of home energy management, as it tells us where the invisible energy comes from and goes away. Based on the sensor installations (distributed sensing or single point sensing), the monitoring approaches can be divided into two categories: intrusive load monitoring (ILM) and non-intrusive load monitoring (NILM). Abubakar et al. [5] formalized the load monitoring concepts and reviewed the approaches for both ILM and NILM. ILM requires the installation of measuring devices at every appliance of interest. In contrast, NILM uses a single-point smart meter to measure the household's total electricity consumption and disaggregates it into individual appliance usage by data mining [12].

'Analyzing & forecasting' layer reprocesses the measured or disaggregated appliance energy consumption details for further information or knowledge. Appliance usage pattern mining can infer users' preferences and quantify their comfort requirement, which is critical for comfort-aware home energy scheduling. Stephen et al. [13] proposed a machine learning solution based on the Kalman filter for online learning of appliance usage characteristics from no prior knowledge. Zhang et al. [14] estimated daily occupant activities from home appliance usages and learned a context-aware personal model to evaluate appliance usage priorities. In [15], several piecewise linear models were applied for quantifying comfort sensitivities of air conditioning systems, electric vehicles, and water heaters in the demand response of a commercial building. Instead of handcraft comfort models, Trinadh et al. [16] estimated the user preference matrix by averaging and standardizing the historical daily appliance ON/OFF states. Rocha et al. [17] applied the K-means clustering to historical daily appliance energy consumptions for characterizing the occupant's appliance usage comfort degree.

Forecasting also plays a vital role in proactive building energy system planning and operation. The advantages are two folds. On the one hand, it can reflect whether the previous understanding of the building energy systems is correct (e.g., model calibration). On the other hand, it can provide additional future information for decision support (e.g., model predictive control). However, obtaining accurate household load forecasts is intractable. The source of the problem is the considerable uncertainty involving human behavior and weather conditions. The bottom-up approach [18,19] and probabilistic load forecasting [6,20] are promising solutions to these issues. In comparison with the top-down approach, the bottom-up method aggregates the forecasts made at a higher spatial granularity level instead of directly forecasting the overall values. Prior research results [18,19,21,22] showed that the measured or disaggregated energy consumption details could improve household

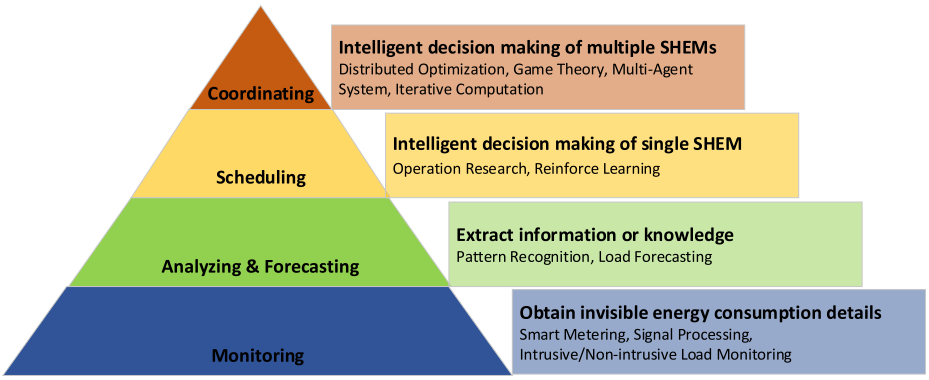

Fig. 1. A taxonomy for smart home energy management.

load forecasting accuracy. On the other hand, probabilistic load forecasting can provide additional information on the variability and uncertainty of future load/PV values. Wang et al. [23] proposed a pinball loss-guided long-short term memory (LSTM) model for individual consumers' probabilistic load forecasting. Zhang et al. [24] proposed a day-ahead probabilistic load forecasting method with probability densities using multiple quantile forecasts and kernel density functions.

Scheduling is the core task for SHEM with intermittent renewable energy resources, flexible demands, and energy storage devices. It allows intricate couplings among local energy generation, consumption, and storage. Generally, the scheduling methods can be characterized into two categories: rule-based control and optimization-based control. The former is straightforward, fast, and widely deployed in practice as it does not need forecasting information and has a less computational burden. The latter takes advantage of the forecasting information and generates optimal control actions by solving an optimization problem.

Coordinating is motivated by the distributed intelligence in the multiagent systems, where multiple intelligent agents' goals are aligned. The neighborhood or community energy system is a typical multiagent system. The SHEM of each house has to address both local objectives and the overall objective or constraints. Prior research results reveal that the coordination of energy management in multiple households can benefit both the utility (i.e., auxiliary services) and the consumers (i.e., cost minimization and comfort maximization). While independently taken decisions may induce undesired effects, such as the rebound peaks, contingencies, and instabilities in the network.

The integration of four layers has arisen interests from researchers recently. Rocha et al. [17] integrated renewable energy forecasting, appliance usage preference quantification, and genetic algorithm (GA)-based home appliance scheduling into a single case study, which has significant practical implications. Nevertheless, the load uncertainties and the coordinating of multiple SHEMs were neglected. Trinadh et al. [16] inferred occupant comfort sensitivities from household non-intrusive load monitoring (NILM) data for comfort-aware appliance scheduling. Hosseini et al. [25] analyzed NILM approaches from the stakeholders' perspective to select employed techniques, such as determining what appliances should be monitored (i.e., the high-power consumption devices and shiftable appliances). Lusis et al. [26] evaluated the impact of different monitoring temporal granularities on household load forecasting. Overall, it is acknowledged that insightful findings can be obtained by combining different layers in a single case study. Nevertheless, there is still no single case study integrating forecasting, analyzing, scheduling, and coordinating layers together to our best knowledge.

2.2. SHEM with residential PV-battery systems

2.2.1. Uncertainty modeling

The optimal operation of residential PV-battery systems is a short-term (day-ahead or real-time) programming problem involving many uncertain parameters (e.g., demands, weather conditions, and electricity prices). Robust optimization and stochastic programming are two popular frameworks to account for uncertainties in optimization problems. The former models the uncertain parameters by uncertain sets and tends to generate risk-averse solutions. Hosseini et al. [27] proposed an adjustable robust optimization model for a residential microgrid comprising active smart users and flexible end-use devices. The uncertainties from demands and renewable power generations were considered by defining the uncertainty sets and incorporating the protection functions into the original deterministic scheduling model. However, multiple users' scheduling problem was formulated in a centralized way, which may be extended in a distributed fashion for scalability. Shi et al. [28] modeled the uncertain EV (dis-)charging behaviors and wind turbine generations by variance intervals and developed a multi-objective adjustable robust optimization model for a microgrid with a group of wind turbines, diesel engines, and grid-responsive electric vehicles to minimize the operation cost and the net environmental emissions. The centralized formulation limits the large-scale deployment, and the robust solution may reduce the economic performance. Since the household demands usually cover a wide range in a day, the uncertainty sets of robust optimizations become pretty broad, producing conservative solutions with inferior economic performance. Thus, this study applied the stochastic programming paradigm for uncertainty modeling. Stochastic programming (optimization) [29] is another modeling framework for uncertainties in optimization problems, where the realizations of uncertain parameters are addressed by scenario analysis. Since the household load forecasting accuracy is still low, the combination of day-ahead (DA) and real-time (RT) markets is a promising solution for leveraging the imperfect household load forecasts and satisfying the uncertain real-time demands. Correa-Florez et al. [30] proposed a two-stage stochastic approach for the day-ahead (DA) operation of home energy management systems with batteries, PV panels, and electric water heaters. The first-stage decision is associated with the DA purchase commitment and the second-stage expected costs are related to the imports/exports imbalance and the battery cycling cost. Though their approach considered both battery degradation effect and uncertain loads and PV generations, the scenarios generated by the 10%,50%,90% quantiles, and their combinations cannot entirely reflect the actual distributions of uncertain loads and PV generations. Liang et al. [15] proposed an optimal demand response framework to enable direct control of demand-side appliances to minimize the total cost and maximize the customers' comfort levels. A two-stage stochastic optimization is modeled by optimizing over the DA electricity market and RT market. Nevertheless, the same real-time buying and selling electricity prices is a strong assumption.

2.2.2. PV power-sharing of multiple SHEMs

As the penetration of distributed PV-battery systems, the SHEM with

energy transaction capability would be the trend. The peer-to-peer (P2P) electricity market, a new proposal for the distributed electricity market's design and operation, has recently raised huge interest from researchers [31,32]. It allows the prosumers with production and storage capabilities to directly share their electric energy and investment. While the schedules of multiple SHEMs must be coordinated for efficient PV power-sharing, considering the heterogenous households' load profiles and energy systems. Since centrally solving the coordinating problem induces computation and communication overhead and privacy concerns, the distributed coordination approaches are promising, such as distributed optimization [31,33–35], game theory [36,37], and marketing mechanism designs. In [34], the alternating direction method of multipliers (ADMM) technique was used for distributed load scheduling to coordinate the operations of multiple home energy management systems in a residential neighborhood. Carli et al. [35] developed a decentralized control approach for residential energy management with renewable energy sharing by extending the ADMM method to a nonconvex and decentralized setting. A deep theoretical analysis was provided for optimality and convergence analysis for the developed algorithm. Nevertheless, the uncertainties in load and renewable energies were not incorporated. Paudel et al. [36] proposed a game-theoretic model for P2P energy trading in a prosumer-based community microgrid. In [37], Mohsenian-Rad proved that as long as the cost functions are increasing and strictly convex, the unique Nash equilibrium of the energy consumption game is the optimal solution of the centralized problem. Scarabaggio et al. [38] proposed a rolling-horizon distributed stochastic control approach for demand side management of a smart grid with multiple active users and a shared wind turbine. The optimization problem was formulated as a noncooperative game and the uncertainty of stochastic wind power is described by defining probability density functions (PDFs) based on the forecast and historical data. Nevertheless, only uncertainties of wind turbines were modeled without considering the uncertainty of household loads and distributed energy sources.

Coordinated PV power-sharing can also be realized by designing marketing mechanisms [37,39–42]. Mohsenian-Rad et al. [37] proposed a pricing and billing model to coordinate each household's energy consumption. The retail prices of electricity are proportional to the time-dependent generation cost, which would depend on how the user and others schedule their consumptions. Yang et al. [40] solved the problem in a parallel distributed way. After receiving the updated prices from the utility, the users could execute their local scheduling algorithm simultaneously. In [41], Yang et al. developed an iterative pricing method for coordinating multi-house appliance scheduling. Penalty terms were induced in the optimization function to penalize significant schedule changes between successive iterations for guaranteeing convergence. Liu et al. [39] developed an energy-sharing model for a microgrid with multiple P2P PV prosumers. A dynamic internal pricing model is formulated for the energy sharing zone based on the local supply–demand ratio (SDR). Zhou et al. [42] proposed two techniques (step length control and learning process involvement) to guarantee the convergence of the iterative pricing methods. Nevertheless, all these power-sharing methods were formulated as an independent problem without integrating the other major functions of SHEM.

3. Methodology

This section presents an integrated SHEM model for operating residential PV-battery systems based on the proposed pyramid taxonomy in Section 2. Since the Monitoring layer can be treated separately, we assume a perfect Monitoring layer and integrate the Analyzing & Forecasting (A&F), Scheduling, and Coordinating layers into one single model. The methodology is organized into four subsections. The first three subsections talk about the A&F layer and Scheduling layers by handling a single-house stochastic energy scheduling problem, incorporating the imperfect forecasts and user preference vectors of shiftable appliances. The final subsection designs a community energy market for coordinated PV power-sharing of multiple households with PV-battery systems and heterogeneous load profiles. Fig. 2 shows an overview of the integrated SHEM model for multiple homes equipped with residential PV-battery systems. The details are presented in later subsections.

3.1. Day-ahead probabilistic household load/PV forecasting

First, we apply the pattern sequence forecasting (PSF) algorithm in [43] for day-ahead probabilistic household loads / PV generations forecasting based on only historical data. This algorithm was developed for univariate time series forecasting and suited to time series forecasting with sequence patterns like daily loads and PV generations.

As shown in Fig. 3, three steps are involved: (historical data) clustering, forecasting, (forecasts) clustering. In step one, the historical data is normalized and split into ordered pieces (by days), and the *K*-means clustering is applied to label each piece. After clustering and labeling, the original time sequence is converted into a series of labels used as input for the forecasting step. In step two, a search window size is selected by cross-validation, and the label subsequence in the window is searched in the label sequence obtained by step one. The label presented just after the matched subsequence is noted in a vector. After the whole searching process ends, the future time series is obtained by averaging the discovered labels' actual values in the vector. In step three, multiple sister forecasters are generated by varying historical training data length (i.e., three-day, one-week, one-month historical data). The forecasts set of these sister forecasters by step two are clustered to generate several typical scenarios with probabilities for usage in the Scheduling layer.

3.2. User preference quantification

Two approaches are usually used to quantify the user comfort degree for home appliance scheduling problems: 1) manual comfort or dissatisfaction functions (named as generative approach) [15,44], and 2) historical data-based preference vectors (called observative approach) [16,17].

We apply the observative approach for single-house appliance scheduling. The historical data-based observative approach estimates the user preference vectors (UPV) from the one-month historical appliance energy consumptions. Fig. 4 is an illustration for obtaining the user preference vector of the washer in an example household, involving three steps as below.

1) Obtain the appliance power profiles by non-intrusive load monitoring or directly measuring the appliances of interest.
2) Formulate the daily appliance state profiles ('1′ for ON mode and '0′ for OFF mode) by binarizing the results of step 1.
3) Calculate the user preference vector by summing, averaging, and normalizing the one-month state profiles from step 2.

As for the community energy management problem with multiple households, we apply the generative approach for simulation convenience. We define the comfort sensitivity function as (1), where $UPV_{k,i}^{app}$ is the user preference value for using appliance k at time slot i, UTR_{lower} and UTR_{upper} denote the lower and upper user-allowed utilization range, PTR_{lower} and PTR_{upper}denote the lower and upper user-preferred utilization range, and i represents the time slot index of one day.

$$UPV_{k,i}^{app} = \begin{cases} \dfrac{i - UTR_{lower}^{k}}{PTR_{lower}^{n} - UTR_{lower}^{n}} & i \in [UTR_{lower}^{k}, PTR_{lower}^{k}) \\ 1 & i \in [PTR_{lower}^{k}, PTR_{upper}^{k}) \\ \dfrac{i - UTR_{upper}^{k}}{PTR_{upper}^{k} - UTR_{upper}^{k}} & i \in [PTR_{upper}^{k}, UTR_{upper}^{k}] \end{cases} \quad (1)$$

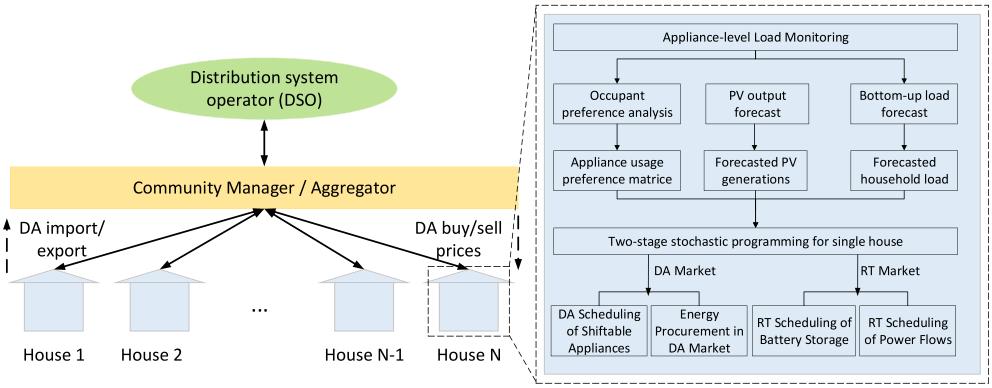

Fig. 2. An integrated SHEM model for residential houses with PV-battery systems for day-ahead (DA) and real-time (RT) stochastic energy scheduling and PV power-sharing.

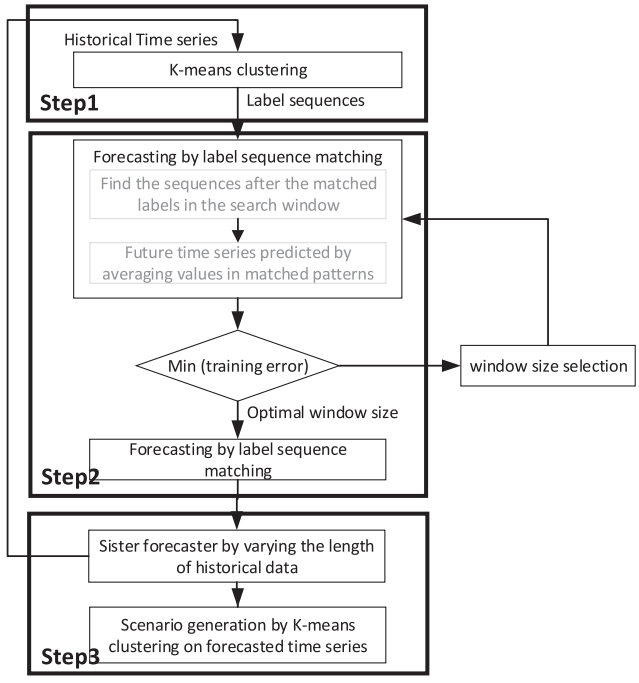

Fig. 3. Diagram of day-ahead probabilistic load/PV forecasting.

The extracted or defined appliance user preference vectors can be used for comfort-aware appliance scheduling later. Note that in this study, we set the length of the control interval as five minutes, and therefore there is a total of 288-time slots for a sample day.

3.3. Two-stage stochastic scheduling for a single house

A retail electricity market is designed first in this subsection, followed by a brief theory related to scenario-based two-stage stochastic programming. Then, the detailed two-stage stochastic programming model is developed based on an AC-coupled grid-connected residential PV-battery system.

3.3.1. The electricity markets

We assume a retail electricity market with both day-ahead (DA) and real-time (RT) energy markets, as shown in Fig. 5. The user could buy or sell electricity from/to the DA market at better prices than that of the RT market to leverage the forecasted information and proactive actions. The deviations of RT energy consumption from the DA planning ones are punished – the real-time buying prices are higher than the day-ahead buying prices, and the real-time selling prices are lower than the day-ahead selling prices.

3.3.1.1. The general two-stage stochastic programming method. Since the energy procurement and real-time scheduling decisions need to be made at different stages and the house demands and PV generations are stochastic, the two-stage stochastic programming (SP) is a promising approach to solve this scheduling problem. The general scenario-based two-stage SP method can be explained as (2).

$$\begin{aligned} &minF(\boldsymbol{x},\ \xi) = f(\boldsymbol{x}) + \sum_{s\in S} p_s \cdot Q(\boldsymbol{x},\ \xi_s) \\ &\text{subject to } \boldsymbol{g}_1(\boldsymbol{x}) \leqslant 0, \boldsymbol{h}_1(\boldsymbol{x}) = 0 \\ &Q(\boldsymbol{x},\ \xi_s) = \min_{\mathbf{y}(\xi_s)} q(\mathbf{y}(\xi_s), \xi_s) \\ &\text{subject to } \boldsymbol{g}_2(\boldsymbol{x},\ \boldsymbol{y}(\xi_s), \xi_s) \leqslant 0,\ \boldsymbol{h}_2(\boldsymbol{x},\ \boldsymbol{y}(\xi_s), \xi_s) = 0, \forall s \in S \end{aligned} \tag{2}$$

where $\mathbf{x}$ is the vector of first-stage decision variables, $\mathbf{y}$ is the vector of second-stage decision variables, ξ represents the uncertain parameters, $s \in S$ is the index of possible realizations of ξ and p_s are the corresponding probabilities. $\mathbf{g}_1(\mathbf{x})$and$\mathbf{h}_1(\mathbf{x})$ are the inequality and equality constraints of the first-stage decision variables. The second-stage optimization model, $Q(\mathbf{x},\ \xi_s) = \min_{\mathbf{y}(\xi_s)} q(\mathbf{y}(\xi_s),\ \xi_s)$, is solved by fixing the first-stage variables and hedging the effect of uncertainty with recourse decisions. The two stages are integrated by link constraints given in $\mathbf{g}_2(\mathbf{x},\ \mathbf{y}(\xi_s),\ \xi_s)$ and $\mathbf{h}_2(\mathbf{x},\ \mathbf{y}(\xi_s),\ \xi_s)$. The goal of SP is to find the policy that is

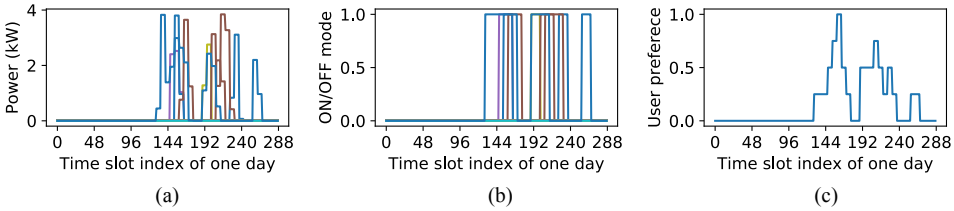

Fig. 4. Illustration for obtaining the user preference vector of washer in an example house: (a) the historical daily appliance energy consumptions; (b) the binarized daily appliance state profiles; (c) the user preference vector.

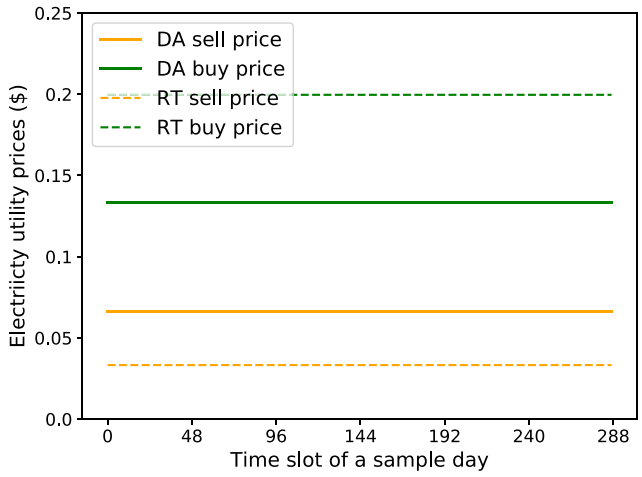

Fig. 5. The retail electricity market with a combination of the DA market and RT market.

feasible for all scenarios and minimize the objective cost function, given uncertain data instances.

3.3.1.2. Mathematic modeling for energy scheduling. We developed the mathematical programming model based on a single household energy system's layout in Fig. 6. The electricity market in Fig. 5 is applied in this study where the house owner could import electricity from and export surplus electricity to the grid in both DA and RT markets.

Fig. 6 shows the physical links of the grid-connected AC-coupled residential PV-battery system and the corresponding power flows. The four components – PV panel, battery, household load, the grid are denoted by R, B, L, C, respectively. Then, we designate, for example, the RT power flows from PV panel to battery at time slot i and scenario s as $y_{i,s}^{RB}(kW)$. Besides, the $x_i^{import}(kW)$and $x_i^{export}(kW)$ denote the imported and exported electricity from the DA retail market. They are constrained as non-negative real values, and they cannot be positive simultaneously. $y_{i,\xi}^{import}(kW)$ and $y_{i,\xi}^{export}(kW)$ denote the imported and exported electricity in the RT market after the uncertain household load and PV generations are realized. They are also constrained as non-negative real values, and they cannot be positive simultaneously. $E_{i,\xi}(kWh)$ denotes the battery energy level, $P_{i,\xi}^{PV}(kW)$and$L_{i,\xi}^{non.}(kW)$ denote the forcing terms of PV output power and the house non-controllable loads at time slot i with uncertainty parameters ξ realized. The single household energy system model is detailed as follows.

1) Household load modeling

First, we assume that the household incorporates a number K of controllable uninterruptable appliances denoted as $\kappa \triangleq \{1,\cdots,k,\cdots,K\}$. We define K column vectors of I binary decision variables $\mathbf{x_k^{app}} \triangleq \{x_{k,1}^{app};\cdots;$ $x_{k,i}^{app};\cdots;x_{k,I}^{app}\}$ representing the ON/OFF states of these shiftable appliances during a day. The energy consumption vectors of these appliances and their aggregation are then obtained by multiplying with their rate powers (3), where $L_i^{shift.}(kW)$ denotes the aggregated energy consumption of shiftable home appliances and $P_k^{rate}(kW)$ denotes the rated power of k^{th} appliance.

$$L_i^{shift.} = \sum_{k=1}^{K} P_k^{rate} \cdot x_{k,i}^{app}, \quad x_{k,i}^{app} \in \{0,1\} \tag{3}$$

We mimic the realistic operation of these shiftable appliances by the transition function (4a), where $u_{k,i}^{app}$ and $d_{k,i}^{app}$ are the binary control variables representing the turning on/off ('1'/'0') actions. Equality constraint (4b) ensures the required operation time length is satisfied within the *UTR*, and the operations are uninterruptable, where $LOT^k(h)$ denotes the required operation time of k^{th} appliance. Equality constraint (4c) provides that the appliances' states and control actions remain "off" outside the *UTR*. Inequality constraint (4d) requires that the turning on/off actions cannot happen simultaneously.

$$x_{k,i+1}^{app} = x_{k,i}^{app} + u_{k,i}^{app} - d_{k,i}^{app}, \; u_{k,i}^{app}, d_{k,i}^{app} \in \{0,1\} \tag{4a}$$

$$\sum_{i\in\Omega^k} x_{k,i}^{app} = \mathrm{LOT}^k, \quad \sum_{i\in\Omega^k} u_{k,i}^{app} = 1, \quad \sum_{i\in\Omega^k} d_{k,i}^{app} = 1, \quad \Omega^k = [UTR_{lower}^k \; UTR_{upper}^k] \tag{4b}$$

$$\sum_{i\in I, i\notin\Omega^k} u_{k,i}^{app} = 0, \; \sum_{i\in I, i\notin\Omega^k} d_{k,i}^{app} = 0, \; \sum_{i\in I, i\notin\Omega^k} x_{k,i}^{app} = 0 \tag{4c}$$

$$u_{k,i}^{app} + d_{k,i}^{app} \leqslant 1 \tag{4d}$$

To calculate the starting and finishing time slots of k^{th}appliance, we define two auxiliary binary variables, $s_{k,i}^{app}$ and $e_{k,i}^{app}$ (5).

$$s_{k,i}^{app} - s_{k,i-1}^{app} \geqslant u_{k,i-1}^{app}, \quad e_{k,i}^{app} - e_{k,i-1}^{app} \geqslant d_{k,i-1}^{app} \tag{5a}$$

$$s_{k,i}^{app} \geqslant s_{k,i-1}^{app}, \quad e_{k,i}^{app} \geqslant e_{k,i-1}^{app}, \quad s_{k,i}^{app}, e_{k,i}^{app} \in \{0,1\} \tag{5b}$$

$$start^k = 288 - \sum_{i=1}^{288} s_{k,i}^{app}, \quad end^k = 288 - \sum_{i=1}^{288} e_{k,i}^{app} \tag{5c}$$

Second, we assume that the household also has some non-controllable loads such as lights and laptops denoted by $L_{i,\xi}^{non.}(kW)$, which is uncertain and dependent on the realization of parameters ξ. Since the shiftable appliances are predictable, the stochastic demands in this study refer to the non-controllable loads. Finally, the total household load is the aggregated energy consumption of shiftable appliances and non-controllable loads. The energy balance for the load node is described as (6).

$$y_{i,\xi}^{RL} + y_{i,\xi}^{BL} + y_{i,\xi}^{CL} = L_{i,\xi}^{non.} + L_i^{shift.} \tag{6}$$

2) PV generation modeling

We also assume each household is equipped with a PV panel with a nominal capacity of $cap^{PV}(m^2)$. The PV outputs $P_{i,\xi}^{PV}(kW)$ are modeled by multiplying the nominal capacity with the PV output of unit panel (1)m^2 as (7a), where $P_{i,\xi}^{PVunit}(kW/m^2)$ is the known forecasted output of a unit PV panel tested under standard conditions during the day. The energy balance for the PV node is described as (7b).

$$P_{i,\xi}^{\mathrm{PV}} = cap^{PV} \cdot P_{i,\xi}^{\mathrm{PVunit}} \tag{7a}$$

$$y_{i,\xi}^{RC} + y_{i,\xi}^{RB} + y_{i,\xi}^{RL} = P_{i,\xi}^{\mathrm{PV}} \tag{7b}$$

The feasible domain of $y_{i,\xi}^{RL}(kW)$ is also related to the household loads and PV generations available:

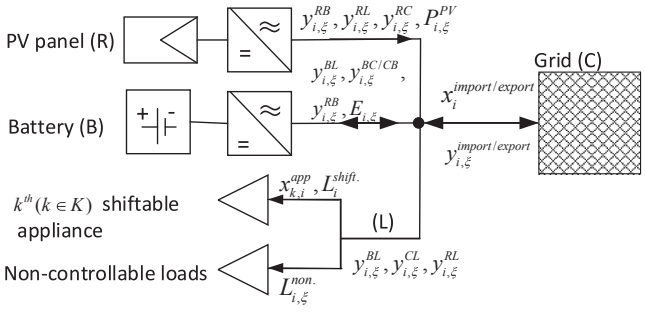

Fig. 6. Single household energy system with energy from the PV panel, battery, and the grid to serve a time-varying household load.

$$0 \leqslant y_{i,\xi}^{RL} \leqslant min(P_{i,\xi}^{\mathrm{PV}}, L_{i,\xi}^{non.} + L_i^{shift.}) \tag{7c}$$

3) Battery dynamic modeling

To model the charging/discharging activities of the battery during a day, we define two real decision variables $y_{i,\xi}^{ch/dis}(kW)$ as (8)

$$\mathrm{y}_{i,\xi}^{dis} = y_{i,\xi}^{BL} + y_{i,\xi}^{BC}, \mathrm{y}_{i,\xi}^{\mathrm{ch}} = y_{i,\xi}^{CB} + y_{i,\xi}^{RB} \tag{8}$$

The battery dynamics can be modeled as the transition function (9a), where $E_{i,\xi}(kWh)$ denotes the battery energy level, η_c and η_d denote the charging and discharging efficiencies, respectively, and $\Delta T(\frac{1}{12}h)$ is the control interval length. Constraint (9b) bounds the battery charge level between the minimum and maximum state of charges SOC_{min} and SOC_{max}, where $cap^B(kWh)$ is the nominal capacity of the installed battery.

$$E_{i+1,\xi} = E_{i,\xi} + [\mathrm{y}_{i,\xi}^{\mathrm{ch}}\eta_c - \mathrm{y}_{i,\xi}^{dis}/\eta_d] \cdot \Delta T \tag{9a}$$

$$cap^B \cdot SOC_{min} \leqslant E_{i,\xi} \leqslant cap^B \cdot SOC_{max} \tag{9b}$$

Moreover, we assume that the charging energy during the day is equal to the discharging energy so that the final energy level is also the initial condition for the next day of the scheduling:

$$\sum_{i=1}^{I}(\mathrm{y}_{i,\xi}^{\mathrm{ch}}\eta_c - \mathrm{y}_{i,\xi}^{dis}/\eta_d) = 0 \tag{9c}$$

Besides, there is usually a maximum (dis-)charging power rate ρ for battery inverters (10a) and the feasible domains of $y_{i,\xi}^{BL}$,$y_{i,\xi}^{RB}$ are also related to uncertain loads and PV generations available (10b), where $L_{i,\xi}^{non.}$ and $L_i^{shift.}$ are the non-controllable and shiftable home loads and $P_{i,\xi}^{PV}$ is the uncertain PV output at time slot i.

$$y_{i,\xi}^{CB} + y_{i,\xi}^{RB} \leqslant \rho, y_{i,\xi}^{BC} + y_{i,\xi}^{BL} \leqslant \rho \tag{10a}$$

$$0 \leqslant y_{i,\xi}^{BL} \leqslant min(\rho, L_{i,\xi}^{non.} + L_i^{shift.}), \quad 0 \leqslant y_{i,\xi}^{RB} \leqslant min(\rho, P_{i,\xi}^{\mathrm{PV}}) \tag{10b}$$

And, the battery cannot simultaneously be charged or discharged from/to the grid (11), where $v_{i,\xi}^B$ is the binary variable for indicating the power flow direction between the battery and the gird:

$$0 \cdot v_{i,\xi}^B \leqslant y_{i,\xi}^{CB} \leqslant \rho \cdot v_{i,\xi}^B, \quad v_{i,\xi}^B \in \{0,1\} \tag{11a}$$

$$0 \cdot (1 - v_{i,\xi}^B) \leqslant y_{i,\xi}^{BC} \leqslant \rho \cdot (1 - v_{i,\xi}^B) \tag{11b}$$

Considering the losses that happened during battery (dis-)charging, the PV output should supply directly to the loads with higher priority than the battery as constrained by (12), where $q_{i,\xi}$ is an auxiliary binary variable for concurrency prevention and $\overline{M}$ is a big positive value for disjunct constraints modeling (i.e., 10000):

$$0 \cdot q_{i,\xi} \leqslant \mathrm{y}_{i,\xi}^{RB} \leqslant \overline{M} \cdot q_{i,\xi}, \quad q_{i,\xi} \in \{0,1\} \tag{12a}$$

$$0 \cdot (1 - q_{i,\xi}) \leqslant \mathrm{y}_{i,\xi}^{BL} \leqslant \overline{M} \cdot (1 - q_{i,\xi}) \tag{12b}$$

4) Supply-demand balance

The supply–demand balance of the whole household is represented as (13). The left-hand side includes the energy supplies from the PV generation, the imported electricity from both DA and RT market, and the battery discharging power $y_{i,\xi}^{dis}$. The right-hand side includes the non-controllable loads, shiftable appliance loads, exported electricity in both DA and RT markets, and the battery charging power $y_{i,\xi}^{ch}$.

$$P_{i,\xi}^{\mathrm{PV}} + x_i^{import} + y_{i,\xi}^{import} + \mathrm{y}_{i,\xi}^{dis} = L_{i,\xi}^{non.} + L_i^{shift.} + x_i^{export} + y_{i,\xi}^{export} + \mathrm{y}_{i,\xi}^{ch} \tag{13}$$

The imported and exported electricity in the RT market can be written as (14). Here, we define two non-negative auxiliary variables $\alpha_{i,\xi}^{buy}(kW), \alpha_{i,\xi}^{sell}(kW)$ for balancing the DA imported electricity with real-time realizations (14a). For example, when x_i^{import} is larger than $y_{i,\xi}^{CL} + y_{i,\xi}^{CB}$, surplus quotas$\alpha_{i,\xi}^{sell}$ are sold to the grid in the RT market. When x_i^{import} is less than $y_{i,\xi}^{CL} + y_{i,\xi}^{CB}$, insufficient demands are satisfied by importing electricity from the RT market with the amount of $\alpha_{i,\xi}^{buy}$. Similarly, $\beta_{i,\xi}^{buy}(kW), \beta_{i,\xi}^{sell}(kW)$ are the non-negative auxiliary variables for balancing the DA exported electricity with the real-time realizations (14b). The real-time imported and exported electricity can thus be calculated by (14c).

$$y_{i,\xi}^{CB} + y_{i,\xi}^{CL} + \alpha_{i,\xi}^{sell} = x_i^{import} + \alpha_{i,\xi}^{buy} \tag{14a}$$

$$y_{i,\xi}^{RC} + y_{i,\xi}^{BC} + \beta_{i,\xi}^{buy} = x_i^{export} + \beta_{i,\xi}^{sell} \tag{14b}$$

$$y_{i,\xi}^{import} = \alpha_{i,\xi}^{buy} + \beta_{i,\xi}^{buy}, \quad y_{i,\xi}^{export} = \alpha_{i,\xi}^{sell} + \beta_{i,\xi}^{sell} \tag{14c}$$

Besides, the upper limits for imported/exported electricity are imposed as (15), where $h_{i,\xi}$ is a binary variable for preventing the simultaneously importing and exporting electricity from the grid.

$$0 \cdot h_{i,\xi} \leqslant y_{i,\xi}^{import} \leqslant L^{import\_upper\_lim} \cdot h_{i,\xi}, \ h_{i,\xi} \in \{0,1\} \tag{15a}$$

$$0 \cdot (1 - h_{i,\xi}) \leqslant y_{i,\xi}^{export} \leqslant L^{export\_upper\_lim} \cdot (1 - h_{i,\xi}) \tag{15b}$$

5) Optimization objective

We formulate the two-stage stochastic scheduling model with two goals. The first-stage goal is to determine the day-ahead power procurement ($x_i^{import}, x_i^{export}$) in the DA electricity market and the operation schedules of shiftable home appliances ($x_{k,i}^{app}, L_i^{shift.}$). These values are determined before the stochastic demands and PV generations are realized. The second goal is to determine the optimal power flows and battery control strategies ($y_{i,\xi}^{import}, y_{i,\xi}^{export}, y_{i,\xi}^{RL}, y_{i,\xi}^{RB}, y_{i,\xi}^{RC}, y_{i,\xi}^{BL}, y_{i,\xi}^{CL}, y_{i,\xi}^{CB}, y_{i,\xi}^{BC}$) during the real-time stage, which dependent on the realization of stochastic demands and PV generations.

To incorporate the impact of appliance scheduling on occupant comfort, we quantify the occupant comfort for using the shiftable appliances at time slot i as (16), where $comfort_i$ is the total comfort value for using shiftable appliances at time slot i, $UPV_{k,i}^{app}$ is the user preference vector obtained in Section 3.2, w_k are the factors weighing the significance of different appliances $k \in \{1,2,\ldots,K\}$.

$$comfort_{\mathrm{i}} = \sum_{k}^{K} \frac{UPV_{k,i}^{app} \cdot x_{k,i}^{app} \cdot w_k}{LOT^k} \tag{16}$$

The final optimization objective is given by:

$$\min_{x \in X, y \in Y} F(x,y) = E[\sum_{i=1}^{I}(\lambda_i^{buy} x_i^{import} - \lambda_i^{sell} x_i^{\mathrm{export}} - \eta \cdot comfort_i) + (\mu_i^{buy} y_{i,\xi}^{import} - \mu_i^{sell} y_{i,\xi}^{\mathrm{export}})] s.t. \qquad (3) - (16) \tag{17}$$

where $\lambda_i^{buy}(\$/kWh)and\lambda_i^{sell}(\$/kWh)$ are the buying and selling prices in the DA market, $\mu_i^{buy}(\$/kWh)and\mu_i^{sell}(\$/kWh)$ are the buying and selling prices in the RT market, η is the weighting factor for trading off between electricity bills and user comfort, whose values are dependent on house owners. We can also write it into the standard two-stage stochastic program as:

$$f(\boldsymbol{x}) = \sum_{i=1}^{I}(\lambda_i^{buy} x_i^{import} - \lambda_i^{sell} x_i^{export} - \eta \cdot comfort_i) \tag{18a}$$

$$q(\boldsymbol{y}(\xi_s), \xi_s) = \sum_{i=1}^{I}(\mu_i^{buy} y_{i,\xi_s}^{import} - \mu_i^{sell} y_{i,\xi_s}^{export}) \tag{18b}$$

The complete formulation of the two-stage stochastic programming model for single-house energy scheduling has been given in Appendix A. The overall problem is a nonconvex optimization problem that consists of determining the $5KI + 3IS$ binary decision variables in $x_{k,i}^{app}, u_{k,i}^{app}, d_{k,i}^{app}, s_{k,i}^{app}, e_{k,i}^{app}, y_{i,\xi}^{B}, h_{i,\xi}, q_{i,\xi}$ and $4I + 2K + 14IS$ non-negative real decision variables in $x_i^{import}, x_i^{export}, L_i^{shift}, comfort_i, start^k, end^k, y_{i,\xi}^{RL}, y_{i,\xi}^{RB}, y_{i,\xi}^{RC}, y_{i,\xi}^{BL}, y_{i,\xi}^{CL}, y_{i,\xi}^{CB}, y_{i,\xi}^{BC}, y_{i,\xi}^{dis}, y_{i,\xi}^{ch}, E_{i,\xi}, \alpha_{i,\xi}^{buy}, \alpha_{i,\xi}^{sell}, \beta_{i,\xi}^{buy}, \beta_{i,\xi}^{sell}$ which minimize the objective function in (17) and meet the $12IS$ bounding constraints in (7c), (9b), (10)-(12), (15), the $5KI$ inequality constraints in (4d), (5a), (5b), and the $I + KI + 10K + 11IS + S$ equality constraints in (3),(4a-c), (5c), (6), (7a, b), (8), (9a,c), (13), (14a-c). In particular, I is the number of time slots during a sample day, K is the number of shiftable appliances in a single house, and S is the number of scenarios for possible realizations of uncertain parameter ξ.

3.4. Energy sharing-enabled multi-house stochastic energy scheduling by iterative internal pricing

In Section 3.3, single houses directly transact energy in the retailer market with fixed DA/RT buying and selling prices. In this subsection, we consider a local energy community formed by a group of households willing to coordinate. Each house is equipped with a distributed PV-battery system and becomes a prosumer (an individual who both consumes and produces electricity). Since the household loads are heterogeneous, the assets of PVs and batteries may be shared among multiple households for efficiency and benefit.

Fig. 7 is the microgrid scheme for PV power-sharing. It is assumed that N active households with shiftable appliances and PV-battery systems of different configurations are willing to coordinate and formulate a local community energy market. The community energy market's initial internal prices are determined by the grid distribution operator or utility companies. A community energy manager collects the DA-imported/exported electricity from each house, calculates the internal buying and selling prices, and broadcasts them to each home. According to the broadcasted prices, the households sequentially change their schedules and report the changes to the community manager. The community manager then updates the internal prices in a repeated process. Note that the internal prices only apply to the DA market for simplification, and the RT market prices are not affected.

The distributed coordination is realized iteratively. At m^{th} coordinating round ($m \in \{1, 2, \cdots, M\}$) each house n ($n \in \{1, 2, \cdots, N\}$) sequentially makes DA energy procurement ($x_{n,i}^{import,(j)}$, $x_{n,i}^{export,(j)}$) through the local SHEM by using the internal prices at j^{th} iteration ($\boldsymbol{\lambda}^{buy,(j)} = \left[\lambda_1^{buy,(j)}, \cdots, \lambda_i^{buy,(j)}, \cdots, \lambda_I^{buy,(j)}\right]$, $\boldsymbol{\lambda}^{sell,(j)} = \left[\lambda_1^{sell,(j)}, \cdots, \lambda_i^{sell,(j)}, \cdots, \lambda_I^{sell,(j)}\right]$, $j \in \{1,2, \cdots, M \times N\}$) and solving the two-stage stochastic scheduling model. After each single household updates the energy schedules, the community manager collects the updated schedules, calculates and broadcasts new internal prices ($\boldsymbol{\lambda}^{buy,(j)}$,$\boldsymbol{\lambda}^{sell,(j)}$) to all users iteratively. Finally, the terminal criteria are checked to decide the final trading internal prices. The detailed algorithm is shown in Table 1, named 'asynchronous iterative pricing' because the users cannot simultaneously change their schedules.

The internal prices updating mechanism is given in Table 2, following Liu's internal pricing model [39], in which the internal prices are functions of the supply–demand ratio (SDR) and the internal selling

Table 1
Asynchronous scheduling iterative pricing algorithm.

Initialize $x_{n,i}^{import,(1)}, x_{n,i}^{export,(1)}, i \in [1,2,\cdots,I], n \in [1,2,\cdots,N]$
Initialize $\boldsymbol{\lambda}^{buy,(1)}, \boldsymbol{\lambda}^{sell,(1)}, j = 1, j \in [1,2,\cdots,M \times N]$
for m = 1 to *M*, **do**
  for n=1 to *N*, **do**
    Local optimization at n^{th} house HEMS center.
    Update DA energy procurement $x_{n,i}^{import}, x_{n,i}^{export}$ from house *n*;
    Update internal prices by **Internal Price Updating Algorithm** in Table 2;
    if $\|\boldsymbol{\lambda}^{buy,(j+1)} - \boldsymbol{\lambda}^{buy,(j)}\|_2 \le \epsilon$ **and** $\|\boldsymbol{\lambda}^{sell,(j+1)} - \boldsymbol{\lambda}^{sell,(j)}\|_2 \le \epsilon$, **then**
      Stop the whole iterative process
    end if
    j = j + 1
  end for
end for
if j≥*MN*, **then**
    The energy-sharing model cannot converge within the required coordinating rounds, and the houses trade with the last iteration's internal prices.
  else
    The internal price is settled as the convergent prices.
  end if

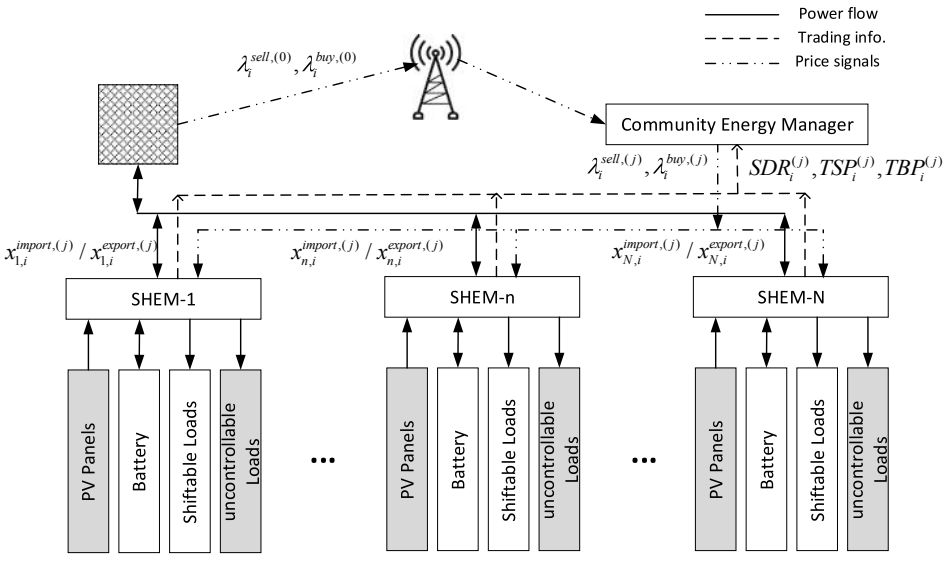

Fig. 7. Scheme of energy and information flows within a community microgrid for multi-house stochastic energy scheduling and power-sharing.

Table 2
Internal prices updating at j^{th} iteration.

Collect DA energy procurements $x_{n,i}^{import}, x_{n,i}^{export}, n \in [1,2,\cdots,N]$ from all houses at j^{th} iteration

Calculate $TSP_i^{(j)}$ and $TBP_i^{(j)}$ by $TSP_i^{(j)} = \sum_{n=1}^{N} x_{n,i}^{export}$, $TBP_i^{(j)} = \sum_{n=1}^{N} x_{n,i}^{import}$

if $TBP_i^{(j)} = 0$ **and** $TSP_i^{(j)} > 0$, **then**:

$$\lambda_i^{sell,(j+1)} = \lambda_i^{buy,(j+1)} = \lambda_i^{sell,(j)}$$

else if $TBP_i^{(j)} = 0$ **and** $TSP_i^{(j)} = 0$, **then**:

$$\lambda_i^{sell,(j+1)} = \lambda_i^{sell,(j)}, \lambda_i^{buy,(j+1)} = \lambda_i^{buy,(j)}$$

else:

$$SDR_i^{(j)} = \frac{TSP_i^{(j)}}{TBP_i^{(j)}}$$

if $0 \le SDR_i^{(j)} \le 1$, **then**:

$$\lambda_i^{sell,(j+1)} = \frac{\lambda_i^{sell,(j)} \cdot \lambda_i^{buy,(j)}}{\left(\lambda_i^{buy,(j)} - \lambda_i^{sell,(j)}\right) \cdot SDR_i^{(j)} + \lambda_i^{sell,(j)}}, \lambda_i^{buy,(j+1)} = \lambda_i^{sell,(j+1)} \cdot SDR_i^{(j)} + \lambda_i^{buy,(j)} \cdot (1 - SDR_i^{(j)})$$

else:

$$\lambda_i^{sell,(j+1)} = \lambda_i^{sell,(j)}, \lambda_i^{buy,(j+1)} = \lambda_i^{sell,(j)}$$

end if

and buying prices at the last iteration (i.e.,$\lambda^{buy,(j)}, \lambda^{sell,(j)}$), as given by (19).

$$\lambda_i^{sell,(j+1)} = \begin{cases} \dfrac{\lambda_i^{sell,(j)} \cdot \lambda_i^{buy,(j)}}{(\lambda_i^{buy,(j)} - \lambda_i^{sell,(j)}) \cdot SDR_i^{(j)} + \lambda_i^{sell,(j)}}, 0 \leqslant SDR_i^{(j)} \leqslant 1 \\ \lambda_i^{sell,(j)}, \ SDR_i^{(j)} > 1 \end{cases}$$

$$\lambda_i^{buy,(j+1)} = \begin{cases} \lambda_i^{sell,(j+1)} \cdot SDR_i^{(j)} + \lambda_i^{buy,(j)} \cdot (1 - SDR_i^{(j)}), 0 \leqslant SDR_i^{(j)} \leqslant 1 \\ \lambda_i^{sell,(j)}, \ SDR_i^{(j)} > 1 \end{cases} \quad (19)$$

$$SDR_i^{(j)} = \frac{TSP_i^{(j)}}{TBP_i^{(j)}}, TSP_i^{(j)} = \sum_{n=1}^{N} x_{n,i}^{export,(j)}, TBP_i^{(j)} = \sum_{n=1}^{N} x_{n,i}^{import,(j)}$$

where $\lambda_i^{sell,(j)}$ and $\lambda_i^{buy,(j)}$ are the internal prices in the DA market at j^{th} iteration and i^{th} time slot, $SDR_i^{(j)}$ denotes the supply–demand ratio of the local community, $TSP_i^{(j)}$ and $TBP_i^{(j)}$ are the total selling and buying power for the community. $x_{n,i}^{import}$ and $x_{n,i}^{export}$ are the imported and exported DA electricity of n^{th} household at time slot i.

4. Simulation setup and data sources

Two set of simulations were conducted to validate the proposed methodology. Simulation I study the single-house stochastic energy scheduling problem, integrating forecasting, appliance usage preference inference, and two-stage stochastic scheduling issues. It applied the sample household loads and PV generations data from IEEE Open Data Set – Consumption [45] and IEEE Open Data Set – PV Generation [46] and the realistic appliance energy consumption data from the SMART* dataset [47]. The parameters for the residential PV-battery system are referred to from literature, as given in Table 3.

Simulation II investigates the coordinated PV power-sharing problems when ten houses are equipped with PV-battery systems and willing to collaborate. The houses are involved in the designed community energy market for local energy transactions and power-sharing. They share the same scheduling model with Simulation I and the same parameters in Table 3. One difference is that the generative approach in Section 3.2 was applied for defining the appliance usage preference vectors due to the large number of appliances involved. The number of shiftable appliances of each house is randomly selected between the range of 5 and 15. The integer PV and battery capacities are chosen randomly within ranges of ($5m^2$, $60m^2$) and ($5kwh$, $20kwh$). The other operational parameters, including PTR, UTR, LOT, w and P^{rate}, are determined similarly. The load and PV generation data of multiple households source from the SMART* dataset [47].

Table 3
Techno-economic parameters of the considered PV-battery model.

Denotations	Description	Value
$\eta_{c/d}$	Battery (dis-)charging efficiency	0.85
ρ	Maximum (dis-)charging power of battery charger	3 kW
SOC_{min}, SOC_{max}	State of charge limits of battery	(0.1,0.9)
$SOC_{initial}, SOC_{end}$	The initial and final state of charges of the battery	(0.5,0.5)

5. Results and discussion

This section introduces the simulation results for both single house stochastic energy scheduling and multi-house coordinated scheduling.

5.1. Simulation I: single-house stochastic energy scheduling

5.1.1. Load / PV forecasting results

The one-month (July 2016) historical data of the SMART* dataset was used for load/PV forecasting. Fig. 8(a) and 9(a) shows the forecasting results for loads and unit PV panel generations of PSF forecaster based on one-month historical data. A set of sister forecasters were generated by varying the length of trained historical data (i.e., three-day, one week, one month) to obtain probabilistic load/PV forecasting. There was a total of 26 sister forecasters for day-ahead load/PV prediction in the final. The corresponding predictions are plotted in Figs. 8(b) and 9(b).

Then, the typical forecast scenarios were produced by applying K-means clustering. Fig. 10 shows the predicted scenarios for household load and unit PV panel production ($1m^2$, rated at 200 W), and Table 4 lists their corresponding probabilities. It is observed that the variations of PV generations are much higher than that of load variations. The former faces issues of sudden output drop and more significant variations. The latter shows a smaller variation in the night but higher variations in the daytime, especially in the evening periods due to the more stochastic human behavior during the occupancy time. Note that since the household load and PV generation are considered independent variables, there were 36 scenarios incorporated into the scheduling model.

5.1.2. Appliance usage preference mining and appliance scheduling

Realistic appliance energy consumption data of a typical household from the SMART* dataset [47] were used to infer appliance usage preference vectors for five shiftable appliances employing the observative technique in Section 3.2. Then, these preference vectors were incorporated into the stochastic scheduling model in Section 3.3. Fig. 11 shows the scheduling results of five appliances and their corresponding preference vectors. It is observed that each appliance is operated at periods with relatively high user preference values to maximize comfort and near to the PV primary output time to reduce electricity bills.

5.1.3. Two-stage energy scheduling

Fig. 12 shows the two-stage stochastic scheduling results for a household with a low PV installation at scenario one. Fig. 12(a) shows the imported and exported electricity in the DA market (upper plot) and the differentiated buying and selling prices in the DA and RT markets (lower plot). It is seen that no surplus energy would be exported to the DA market due to the low local generations, and most imported electricity is intended for the usage of the shiftable appliance loads and the stable fixed load in the morning and evening periods. Fig. 12(b) shows the balance of flowing-in power and flowing-out power for the load node. It is seen that the grid, PV generator, and battery work together to support the fixed and shiftable loads. Fig. 12(c) shows the balance of

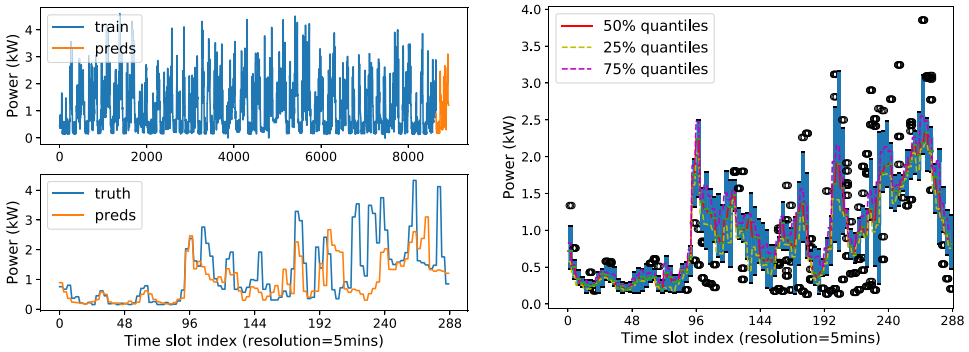

(a) (b)

Fig. 8. Load forecasts (a) the sister forecaster's forecasts with one-month training data; (b) the forecasts set by all the sister forecasters.

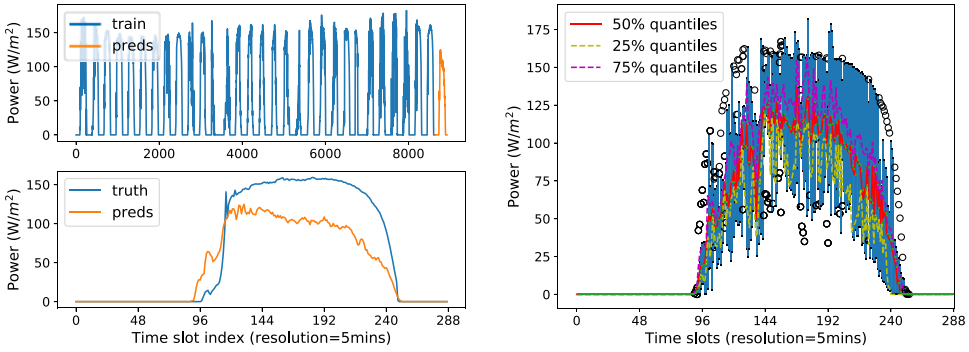

(a) (b)

Fig. 9. Unit PV panel generation forecasts (a) the sister forecaster's forecasts with one-month training data; (b) the forecasts set by all the sister forecasters.

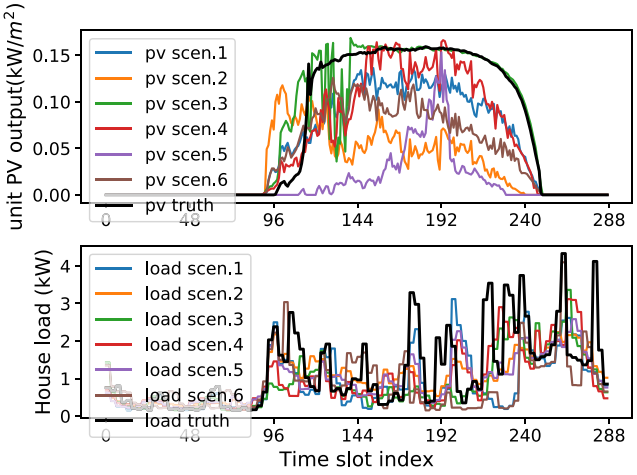

Fig. 10. Typical scenarios for household load and PV generation forecasts.

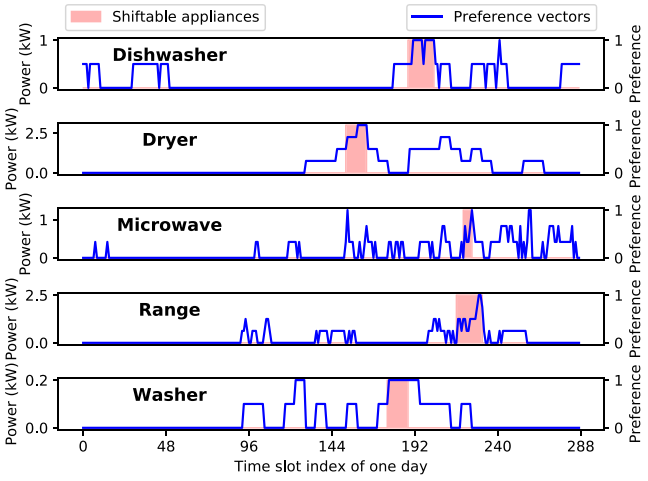

Fig. 11. Shiftable appliances scheduling with appliance usage preference vectors.

Table 4
Probabilities of forecasted scenarios.

Scenario	1	2	3	4	5	6
PV probability	0.3846	0.0769	0.1154	0.1154	0.1538	0.1538
Load probability	0.1154	0.3462	0.1154	0.0769	0.3077	0.0384

flowing-in power and flowing-out power for the PV node. It is seen that the PV generations are used for direct consumption of house load, battery charging, and exporting to the grid. Fig. 12(d) shows the supply–demand balance of the system. The demand-side includes fixed load, shiftable loads, exported electricity in both DA and RT market, and the battery charging energy. The supply-side consists of the PV generations, the imported electricity from the DA market, and the battery discharging power. There is no imported electricity in the RT market due to its high buying prices. Considerable demand is supplied by battery discharging energy. Most PV energy supplies to the house load directly or stores in the battery and only a little PV electricity is exported to the RT market due to the low selling prices.

Fig. 13 shows the two-stage stochastic scheduling results for a household with a high PV installation at scenario one. A significant difference can be observed compared with Fig. 12. In Fig. 13(a), only a little electricity is imported in advance for supporting the high and

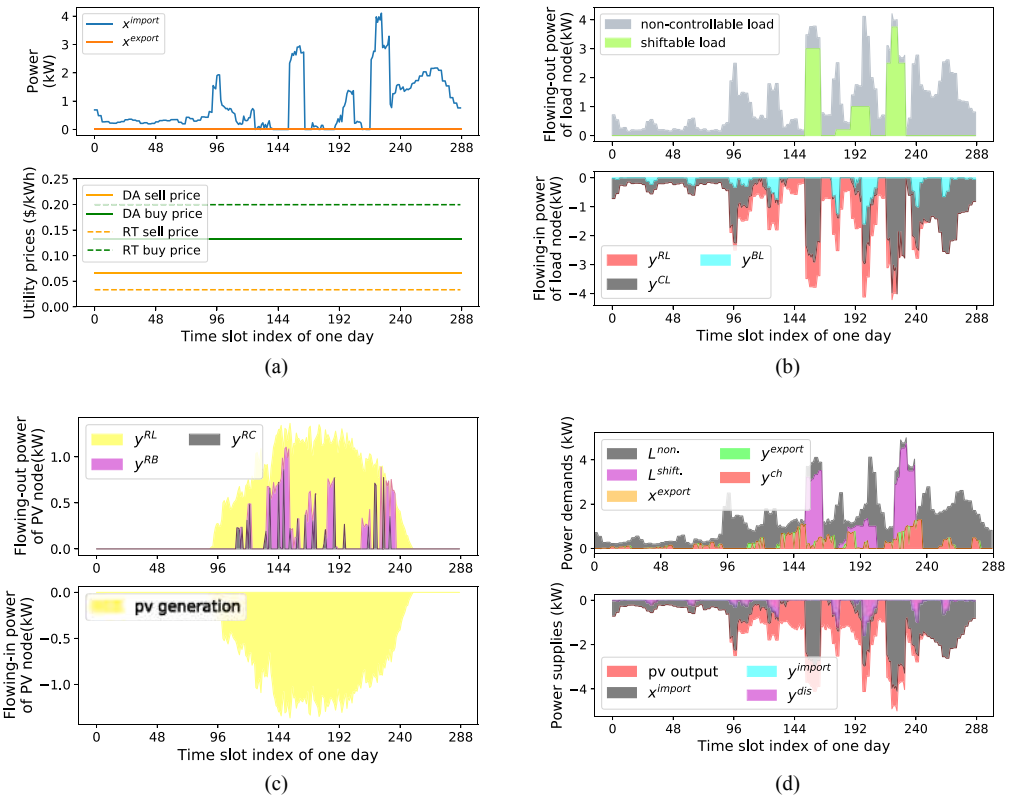

Fig. 12. Scheduling results for low PV-installation household ($cap^B = 10kWh, cap^{PV} = 10m^2$, scenario one) (a) first-stage day-ahead energy procurement, and differentiated pricing scheme; (b) flowing-in and flowing-out powers of load node; (c) flowing-in and flowing-out powers of PV node; (d) balancing of energy demands and supplies; (positive and genitive values denote power flows with different directions).

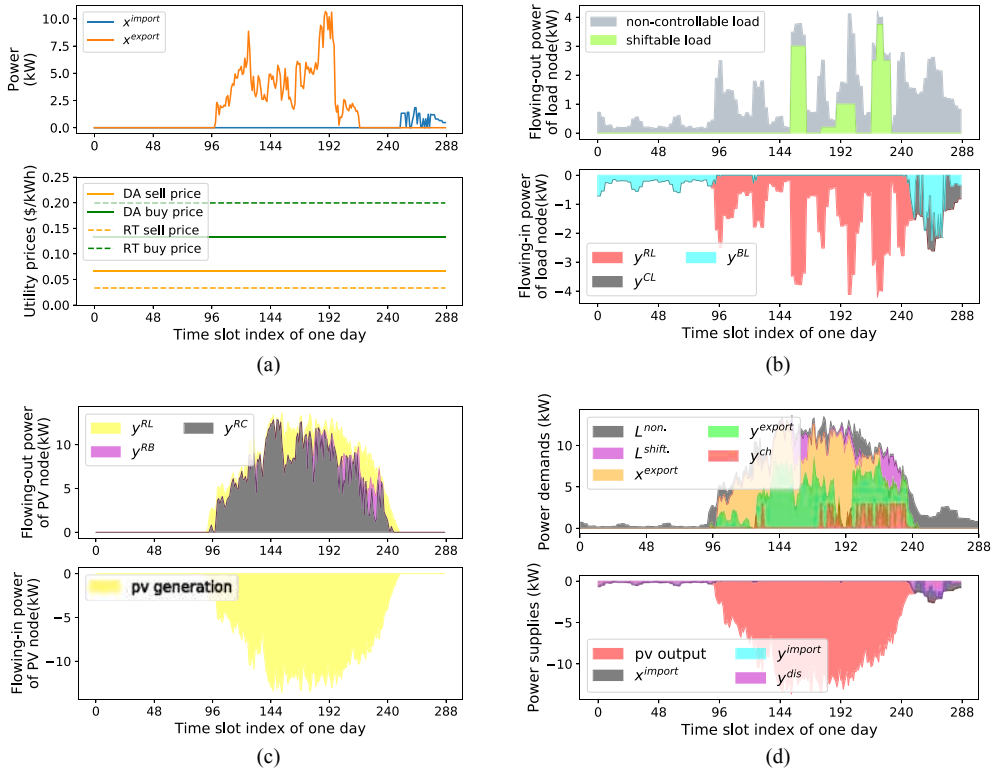

Fig. 13. Scheduling results for high PV-installation household ($cap^B = 10kWh, cap^{PV} = 100m^2$, scenario one) (a) first-stage day-ahead energy procurement, and differentiated pricing scheme; (b) flowing-in and flowing-out powers of load node; (c) flowing-in and flowing-out powers of PV node; (d) balancing of energy demands and supplies; (positive and genitive values denote power flows with different directions).

predictable evening load. Though the morning load is also stable and predictable, there is no imported electricity in that periods due to the battery discharging actions. Meanwhile, a large amount of electricity is exported to the DA market in the daytime due to the high local generations. In Fig. 13(b)(c), the flowing-in and flowing-out power of load and PV node share the same components as Fig. 12(a)(c). However, the gird-side load supply reduces, and the exported PV electricity to the DA market increases significantly. In Fig. 13(d), the exported electricity to both DA and RT market take up a large proportion. A large proportion of PV electricity is exported to the RT market instead of the DA market, which indicates that a predictable PV generation is significant in our retail electricity market.

Fig. 14 shows the battery control strategies under two situations: low PV installation and high PV installation. In the low PV installation case (left picture), part of the battery energy is supplied to the local load. The battery is then recharged to its initial SOC level using power from surplus solar energy and the grid-side energy. It is interesting that y^{CB} is not zero, though the buying prices in the RT market are much higher. This may because the imported electricity in the DA market has a surplus, and it would be better to store the surplus imported electricity than re-selling to the RT market. In the high PV installation case (right picture), the battery is charged in the daytime using the surplus solar energy and discharged in the early morning and evening to support the household load. It is also observed that the final values of both SOC curves keep the same as the initial values.

In the stochastic programming field, three solutions are usually defined and compared together to verify the value of the stochastic solutions: wait-and-see solution (*WS*), recourse problem solution (*RP*), and the expectation of the expected value solution (*EEV*). In our context, The RP solution is the solution of our two-stage scheduling model. The detailed definitions and calculation methods of another two solutions are described in Appendix B for space concerns. Then, we calculated the three solutions with different PV sizes (the battery capacity is always 10 kWh).

In Table 5 and Fig. 15, we can observe that the *RP* solutions always lie between the values of *WS* and *EEV* solutions and satisfy the relations of $WS \leq RP \leq EEV$. The first relation $WS \leq RP$ states that it is always better to get the prior information of uncertainties. The second relation $RP \leq EEV$ envisions that it is always better to have recourse actions after the uncertainties are revealed than the results of merely averaging uncertainties [29,48]. Therefore, we now verified our two-stage stochastic scheduling model's effectiveness and the value of modeling uncertainties. Note that the first-row values in Table 5 denote the *Comfort* values of appliance scheduling in the RP solutions, relatively independent of the PV sizes. The other three rows' values are obtained by subtracting the *comfort of RP* from the objective values.

5.1.4. Comparison between stochastic scheduling and rule-based scheduling

To validate our model's usefulness, we compare our method (RP approach) with the basic rule-based energy dispatch (RBC) strategy (detailed in Appendix C). The RBC method assumes that the user cannot participate in the DA market, and all relevant variables are determined in real-time. The load is filled with PV, battery, and grid priorities, and the battery is only used to store surplus PV energy in the noon and release energy in the evening periods. In contrast, the RP method could determine the amount of buying and selling powers in both DA and RT markets and the RT battery (dis-)charging actions. Both approaches apply the same realistic load and unit PV output profiles, as shown in Fig. 10 (black curves).

Fig. 16 shows the cost values of two approaches in a sample day under different PV sizes ($cap^{PV} = 5, 10, 25, 50, 75, 100 m^2$) and the same battery sizes ($cap^{B} = 10kWh$). It is found that the RP method can achieve less or comparable cost values than the RBC method in most cases. However, when the PV size equals $25m^2$, the RBC solution has a lower cost value, though not so significant. To interpret this result, we plot the DA/RT importing/exporting power profiles and the battery (dis-) charging powers of two approaches under the PV size of $25m^2$, as shown

Table 5
The objective values of different solutions (*WS*, *RP*, and *EEV*) under different PV sizes.

PV size (m^2)	5	10	25	50	75	100
Comfort of RP(-)	3.93	3.93	3.58	3.53	3.93	3.93
WS ($)*	33.36	25.71	5.36	−18.05	−39.39	−60.22
EEV ($)*	35.82	29.11	11.57	−5.22	−18.8	−30.86
RP ($)*	35.58	28.61	10.24	−7.1	−21.48	−35.5

'-' means dimensionless, and '*' denotes the cost values obtained by subtracting *Comfort of RP* from the objective values.

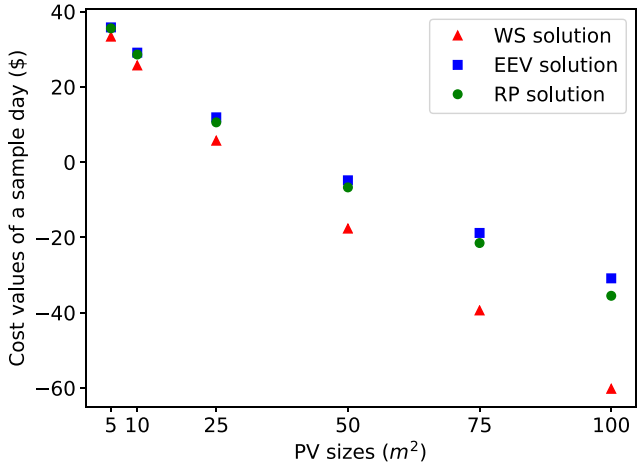

Fig. 15. The values of WS, RP, and EEV solutions under different PV sizes.

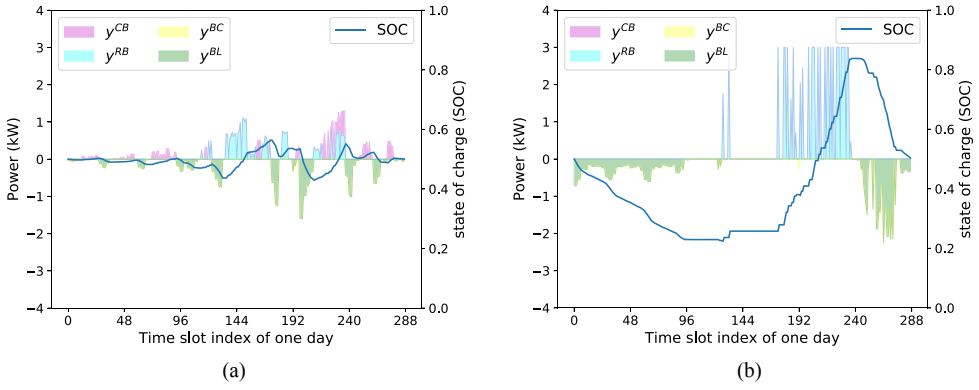

Fig. 14. Battery control strategies under (a) low PV-installation and (b) high PV-installation.

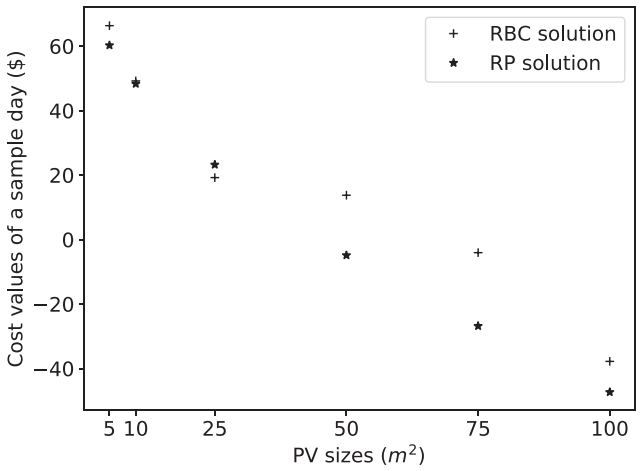

Fig. 16. Cost values of RBC and RP approaches in a sample day under different PV sizes.

in Fig. 17. Comparing Fig. 17(a) and 17(c), the RP method exports more surplus PV energy to the RT market at low prices in the noon and imports more electricity from the RT market at high prices in the evening than that of the RBC approach. Fig. 17(d) shows the battery was never charged to its full capacity for the RP method. In contrast, the RBC approach can charge to its full capacity using the surplus solar energy in the noon and release them to support the evening load, as shown in Fig. 17(b). It is concluded that the buffering potential of the battery is fully exploited in the RBC method. The inefficient usage of batteries in the RP method may offset the benefit of participating in the DA market.

To enhance the economic performance, we hybrid the RP method with the RBC method for leveraging the benefit of participating in the DA market and the battery buffering potential, as shown by Fig. 27 in Appendix D. The hybrid approach utilizes the RP method for DA power procurements and the RBC method for battery (dis-)charging control based on the original RP solutions. Fig. 18 plots the DA/RT importing and exporting power profiles and battery (dis-)charging profiles for the hybrid approach with PV size of $25m^2$. Comparing Fig. 18(a) and 17(c), a large proportion of surplus PV energy was stored in the battery in the noon instead of selling them in the RT market at low prices. Then, these stored energies were released in the evening periods to avoid buying electricity from the RT market at high prices. Thus, the cost values are significantly reduced. Comparing Fig. 18(a) and 17(a), a large portion of the morning and evening loads were supplied by the DA-imported electricity, which induces less costs than importing from the RT market. Fig. 19 plots the cost values of three approaches (the RP, RBC, hybrid approaches) in terms of different PV sizes. It is observed that the hybrid approach can achieve the least cost values under all cases.

5.2. Simulation II: PV power-sharing of multiple households

Fig. 20 shows the evolutional DA internal buying (green) and selling (yellow) prices obtained by the asynchronous scheduling and iterative pricing method. Each price trace fades as the iteration goes on. It is seen that as the iterations go on, the prices can converge to stable tracks. Compared to the retail market, the stable internal buying price tracks are much lower than the original buying prices. The stable internal selling price tracks are higher than the original ones in the daytime. Thus, all electricity consumers and prosumers can expectedly benefit from this community energy market.

Fig. 21 plots the Euclidean distances of consecutively updated selling/buying prices and the total microgrid objective (cost) values for $M \times N = 10 \times 10 = 100$ iterations (M coordinating rounds for N houses). It is seen that the price deviations between consecutively updated internal prices reduced quickly at first and then the distances fluctuated around \$0.1. The total cost values also reduce dramatically at first and get stable after the initial big fluctuations. The determination of the final trading prices is dependent on the terminal conditions. Note that Fig. 20 is obtained for a divergent case with the terminal condition of $\max(\|\boldsymbol{\lambda}^{buy,(j+1)} - \boldsymbol{\lambda}^{buy,(j)}\|_2$,

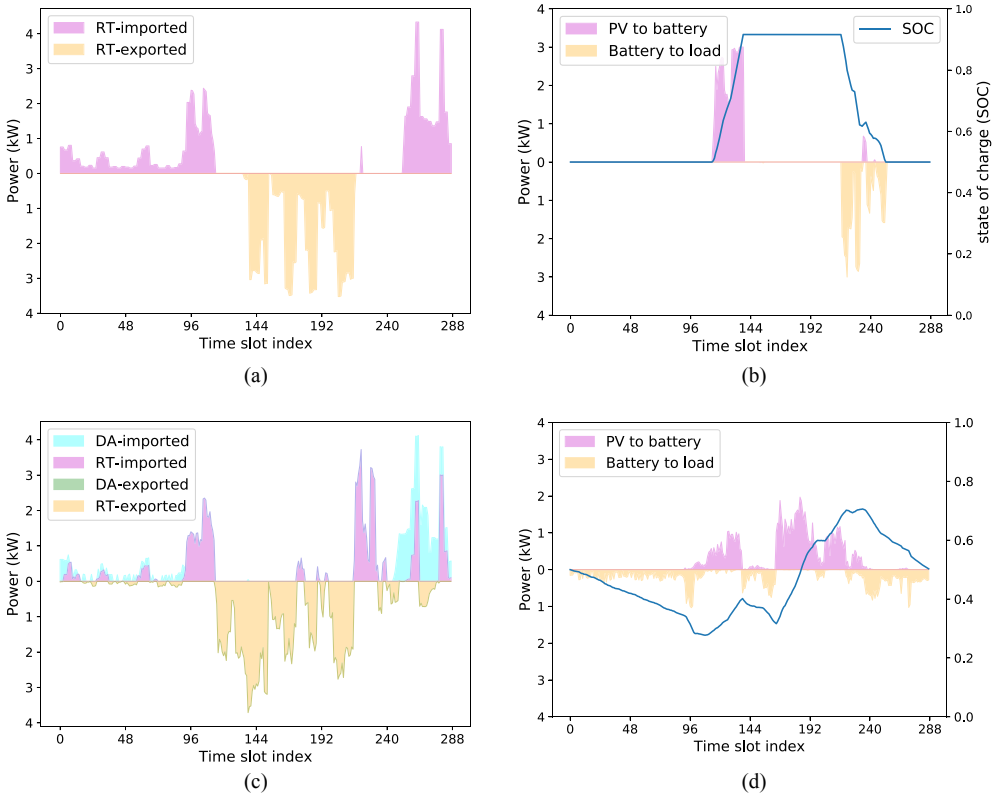

Fig. 17. DA/RT importing and exporting power profiles and battery (dis-)charging profiles for RBC approach (a)(b) and RP approaches (c)(d) with PV size of.$25m^2$

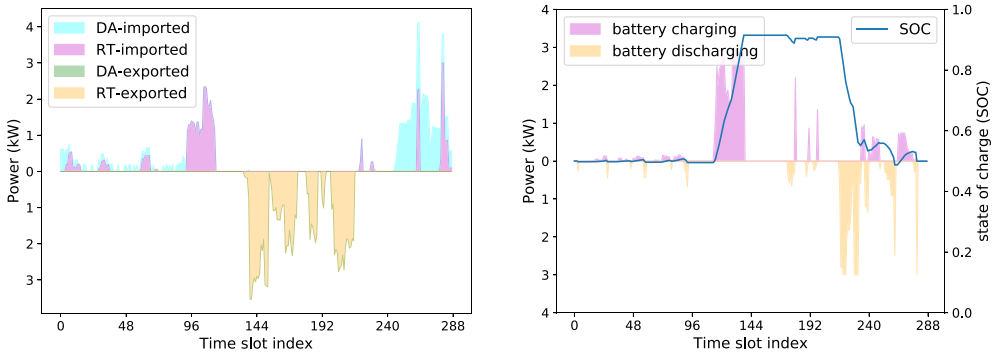

Fig. 18. DA/RT importing and exporting power profiles (a) and battery (dis-)charging profiles (b) for the hybrid approach with PV size of.25m^2

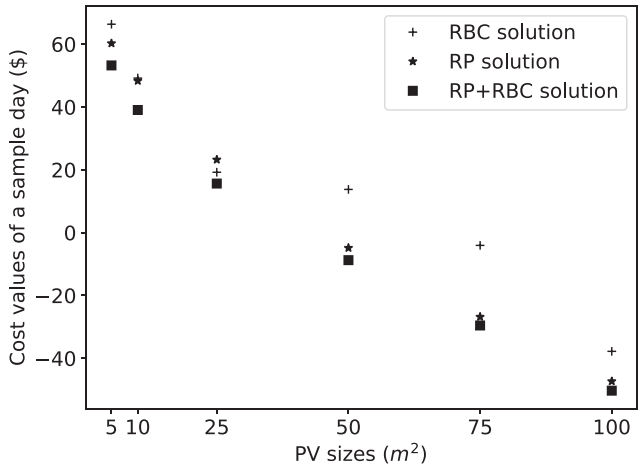

Fig. 19. Cost values of the RBC, RP, and hybrid approaches in a sample day under different PV sizes.

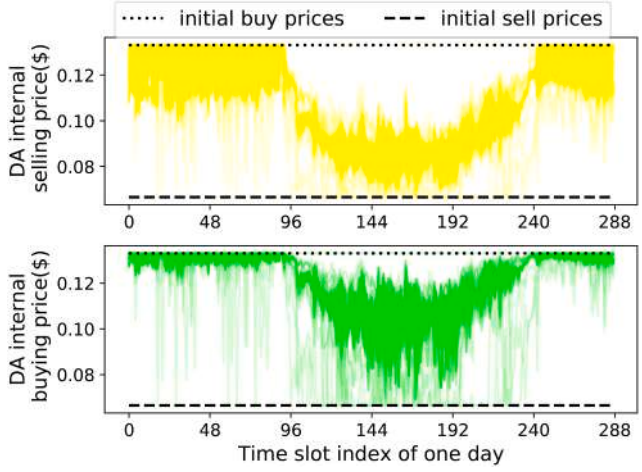

Fig. 20. Evolutional DA internal prices for a microgrid with ten households.

$\|\lambda^{sell,(j+1)} - \lambda^{sell,(j)}\|_2) \leq 0.01$. If we set the terminal condition as 0.1, the algorithm would converge within ten iterations. Besides, the final trading prices can also be decided with the help of market regulations. For example, the internal prices must be determined within limited iterations or periods. Since the coordinating algorithm is not based on a global optimization problem, this algorithm's optimality is not guaranteed. The authors intend to leave the deep theoretical convergence and optimality analysis of the distributed algorithm for feature work. The readers may refer to [37,40,49] for more information about this algorithm.

Fig. 22 shows the cost values of ten houses in the microgrid with selfish and coordinated scheduling. The 'selfish' households were charged by the initial buying and selling prices. The 'coordinated' homes were billed by the settled internal buying and selling prices (determined as the last iteration prices). The positive bars denote the cost, and the negative bars indicate the revenue. It is observed that coordinating the multiple prosumers can reduce the overall cost, and each household can benefit from the power-sharing by either selling electricity at higher prices or buying electricity at lower prices.

However, the scalability to a large number of users is limited due to each user's sequential scheduling. Fortunately, the general shape of internal prices can be stable within a few iterations, even though the involved number of households is large. For example, for a microgrid with 100 end-users, each user's sequential scheduling may take a long time for one coordinating round (nearly half a day on a laptop with Intel (R) Core TM i7-7700HQCPU @ 2.80 GHz). Nevertheless, the general shapes of internal prices and the errors between consecutively updated prices become stable within fifty iterations, as shown in Fig. 23. Since the internal pricing is applied to the DA market, the maximum coordinating time is a whole day. Thus, the maximum number of household members can be estimated as 200 houses if the iterative process goes on for at most one coordinating round. The possible solutions to improve the scalability may include synchronous or semi-asynchronous scheduling. The former uses synchronous scheduling and introduces penalty factors on the changes of consecutively updated schedules [40]. The latter combines synchronous and asynchronous scheduling by clustering similar users into representative groups and doing synchronous scheduling within intra-groups and asynchronous scheduling between inter-groups.

6. Conclusion and future development

This paper proposed a specialized taxonomy for integrated designs and operations of smart home energy management systems. The primary functional layers are organized by a pyramid starting from basic to advanced topics: monitoring, analyzing & forecasting, scheduling, and coordinating. Guided by the taxonomy, an integrated SHEM model is developed for energy management of smart homes with grid-connected residential PV-battery systems under uncertain loads and PV generations, which is the core contribution of this paper.

First, we apply a scalable and robust algorithm - Pattern Sequence Forecasting for day-ahead probabilistic household load and PV forecasting relying on only historical measurement. Second, we quantify the users' comfort preference for comfort-aware appliance scheduling by estimating user preference vectors from historical daily appliance energy consumption data. Third, we develop a two-stage stochastic programming model for single households' energy scheduling with PV-battery systems, incorporating the probabilistic load / PV forecasts

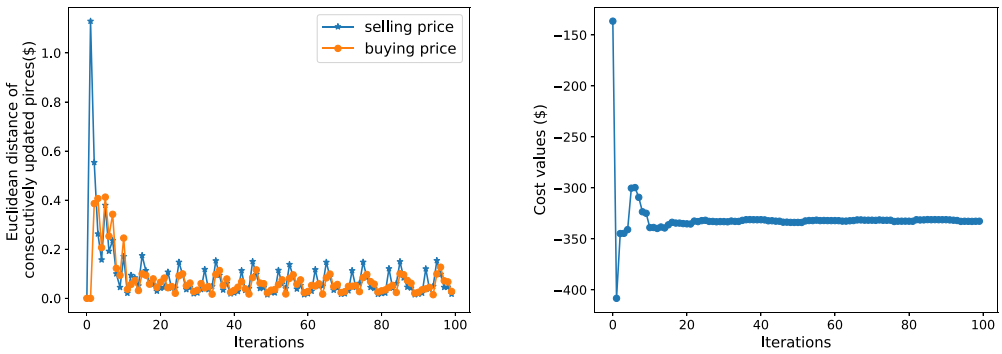

(a) (b)

Fig. 21. Euclidean distances of consecutively updated prices (a) and total cost alues (b) for a microgrid with ten households under ten coordinating rounds.

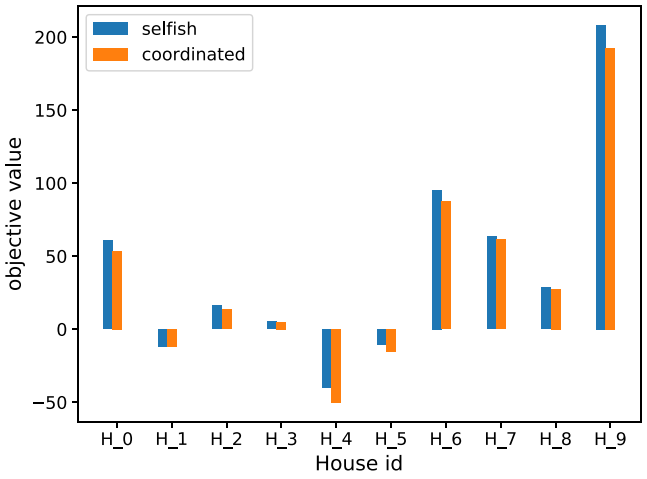

Fig. 22. Cost values of ten houses in the microgrid with selfish and coordinated scheduling, respectively.

and user preference vectors of shiftable appliances. The first stage determines the optimal day-ahead (DA) energy procurement and the DA scheduling of shiftable appliances. The second stage optimizes the real-time (RT) power flows and battery (dis-)charging actions after the uncertain household loads and PV generations are realized. By designing a retail electricity market with DA and RT markets, the accuracy improvement of forecasting is motivated by the scheduling layer since the RT market's worse prices will punish the inaccurate forecasts. Finally, we propose a distributed coordinating approach for power-sharing among multiple households with PV-battery systems through establishing a community energy market. The distributed power-sharing is realized by iteratively updating internal prices and asynchronously rescheduling each home, which reduces the computational burden without revealing private information. Numerical simulations based on realistic datasets validated the integrated SHEM model's effectiveness and the practical guidance meaning of the SHEM pyramid taxonomy. The value of modeling stochastic load and PV generations is also verified. Compared with the basic rule-based energy dispatch strategy, the two-stage stochastic scheduling model could achieve less or comparable cost values by leveraging the benefit of participating in the DA market. A hybrid of both methods could enhance the economic performance by fully exploiting the battery buffering potential. The coordinated scheduling can benefit each household by sharing PV and battery investments for revenue or trading with local small prosumers for cost reductions.

Overall, this paper provides a pyramid taxonomy for standard-based development and implementation of SHEM and an integrated SHEM model for residential communities with distributed PV-battery systems. Future development may include the deep theoretical analysis of the distributed power-sharing algorithm's convergence and optimality properties, the extension to interruptible thermal appliances and electric vehicles, and other uncertainty modeling methods like robust optimization.

CRediT authorship contribution statement

Zhuang Zheng: Conceptualization, Methodology, Formal analysis, Writing - original draft. **Zhankun Sun:** Conceptualization, Methodology, Writing - review & editing. **Jia Pan:** Writing - review & editing. **Xiaowei Luo:** Supervision, Methodology, Writing - review & editing.

Declaration of Competing Interest

The author declare that there is no conflict of interest.

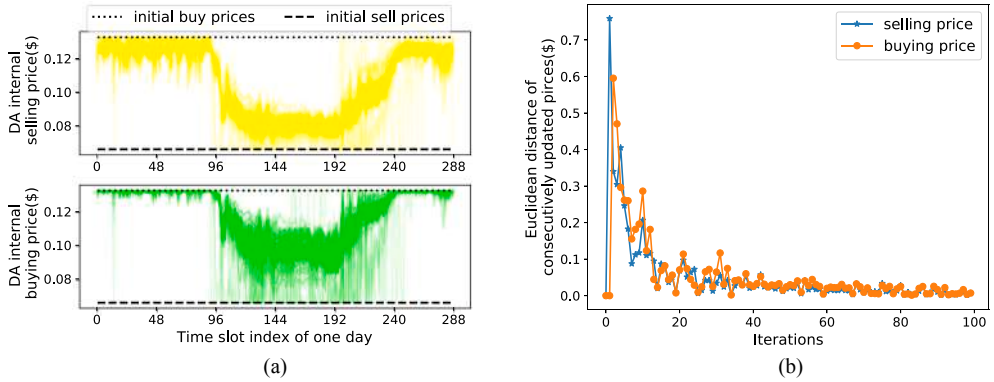

(a) (b)

Fig. 23. Evolutonal DA internal prices (a) and Euclidean distances of consecutively updated prices(b) for a microgrid with 100 households under one coordinating round.

Appendix A. . Two-stage stochastic scheduling model

$$\min_{x\in X, y\in Y} F(x,y) = \mathbb{E}[\sum_{i=1}^{I}(\lambda_i^{buy} x_i^{import} - \lambda_i^{sell} x_i^{export} - \eta\cdot comfort_i) + (\mu_i^{buy} y_{i,\xi}^{import} - \mu_i^{sell} y_{i,\xi}^{export})]$$

$$y_{i,\xi}^{RL} + y_{i,\xi}^{BL} + y_{i,\xi}^{CL} = L_{i,\xi}^{non.} + L_i^{shift.}$$

$$y_{i,\xi}^{RC} + y_{i,\xi}^{RB} + y_{i,\xi}^{RL} = P_{i,\xi}^{\mathrm{PV}}$$

$$P_{i,\xi}^{\mathrm{PV}} = cap^{PV}\cdot P_{i,\xi}^{\mathrm{PVunit}}$$

$$P_{i,\xi}^{\mathrm{PV}} + x_i^{import} + y_{i,\xi}^{import} + \mathrm{y}_{i,\xi}^{dis} = L_{i,\xi}^{fix} + L_i^{shift} + x_i^{export} + \mathrm{y}_{i,\xi}^{export} + \mathrm{y}_{i,\xi}^{ch}$$

$$\mathrm{y}_{i,\xi}^{dis} = y_{i,\xi}^{BL} + y_{i,\xi}^{BC}$$

$$\mathrm{y}_{i,\xi}^{ch} = y_{i,\xi}^{CB} + y_{i,\xi}^{RB}$$

$$y_{i,\xi}^{import} = \alpha_{i,\xi}^{buy} + \beta_{i,\xi}^{buy}$$

$$y_{i,\xi}^{export} = \alpha_{i,\xi}^{sell} + \beta_{i,\xi}^{sell}$$

$$y_{i,\xi}^{CB} + y_{i,\xi}^{CL} + \alpha_{i,\xi}^{sell} = x_i^{import} + \alpha_{i,\xi}^{buy}$$

$$y_{i,\xi}^{RC} + y_{i,\xi}^{BC} + \beta_{i,\xi}^{buy} = x_i^{export} + \beta_{i,\xi}^{sell}$$

$$E_{i+1,\xi} = E_{i,\xi} + [(y_{i,\xi}^{CB} + y_{i,\xi}^{RB})\eta_c - (y_{i,\xi}^{BC} + y_{i,\xi}^{BL})\Big/\eta_d]\cdot\Delta T$$

$$\sum_{i=1}^{I}((y_{i,\xi}^{CB} + y_{i,\xi}^{RB})\eta_c - (y_{i,\xi}^{BC} + y_{i,\xi}^{BL})\Big/\eta_d) = 0$$

$$cap^B\cdot SOC_{min} \leqslant E_{i,\xi} \leqslant cap^B\cdot SOC_{max}$$

$$0\cdot v_{i,\xi}^B \leqslant y_{i,\xi}^{CB} \leqslant \rho\cdot v_{i,\xi}^B,\ v_{i,\xi}^B \in \{0,1\}$$

$$0\cdot(1 - v_{i,\xi}^B) \leqslant y_{i,\xi}^{BC} \leqslant \rho\cdot(1 - v_{i,\xi}^B)$$

$$0 \leqslant y_{i,\xi}^{BL} \leqslant min(\rho, L_{i,\xi}^{non.} + L_i^{shift.}), \qquad 0 \leqslant y_{i,\xi}^{RB} \leqslant min(\rho, P_{i,\xi}^{\mathrm{PV}})$$

$$y_{i,\xi}^{CB} + y_{i,\xi}^{RB} \leqslant \rho,\ y_{i,\xi}^{BC} + y_{i,\xi}^{BL} \leqslant \rho$$

$$0\cdot h_{i,\xi} \leqslant y_{i,\xi}^{import} \leqslant L^{import\_upper\_lim}\cdot h_{i,\xi}, \qquad h_{i,\xi} \in \{0,1\}$$

$$0\cdot(1 - h_{i,\xi}) \leqslant y_{i,\xi}^{export} \leqslant L^{export\_upper\_lim}\cdot(1 - h_{i,\xi})$$

$$0\cdot q_{i,\xi} \leqslant \mathrm{y}_{i,\xi}^{RB} \leqslant \overline{M}\cdot q_{i,\xi}, \qquad q_{i,\xi} \in \{0,1\}$$

$$0\cdot(1 - q_{i,\xi}) \leqslant \mathrm{y}_{i,\xi}^{BL} \leqslant \overline{M}\cdot(1 - q_{i,\xi})$$

$$0 \leqslant y_i^{RL} \leqslant min(P_{i,\xi}^{\mathrm{PV}}, L_{i,\xi}^{non.} + L_i^{shift.})$$

$$comfort_{\mathrm{i}} = \sum_{k}^{K}\frac{PV_{k,i}^{app}\cdot x_{k,i}^{app}\cdot w_k}{LOT^k}$$

$$L_i^{shift.} = \sum_{k=1}^{K} P_k^{rate}\cdot x_{k,i}^{app}, \qquad x_{k,i}^{app} \in \{0,1\}$$

$$x_{k,i+1}^{app} = x_{k,i}^{app} + u_{k,i}^{app} - d_{k,i}^{app}, \qquad x_{k,i}^{app}, u_{k,i}^{app}, d_{k,i}^{app} \in \{0,1\}$$

$$\sum_{i\in\Omega^k} x_{k,i}^{app} = \mathrm{LOT}^k,\ \sum_{i\in I, i\notin\Omega^k} x_{k,i}^{app} = 0, \qquad \Omega^k = [UTR_{lower}^k\ UTR_{upper}^k]$$

$$\sum_{i\in I, i\notin\Omega^k} u_{k,i}^{app} = 0, \qquad \sum_{i\in I, i\notin\Omega^k} d_{k,i}^{app} = 0\ , \qquad \sum_{i\in\Omega^k} u_{k,i}^{app} = 1, \qquad \sum_{i\in\Omega^k} d_{k,i}^{app} = 1$$

$$u_{k,i}^{app} + d_{k,i}^{app} \leqslant 1, \qquad s_{k,i}^{app} - s_{k,i-1}^{app} \geqslant u_{k,i-1}^{app}, \qquad e_{k,i}^{app} - e_{k,i-1}^{app} \geqslant d_{k,i-1}^{app}$$

$$s_{k,i}^{app} \geqslant s_{k,i-1}^{app}, \qquad e_{k,i}^{app} \geqslant e_{k,i-1}^{app}, \qquad s_{k,i}^{app}, e_{k,i}^{app} \in \{0,1\}$$

$$start^k = 288 - \sum_{i=1}^{288} s_{k,i}^{app}, \qquad end^k = 288 - \sum_{i=1}^{288} e_{k,i}^{app}$$

Appendix B. The value of stochastic solutions

1) Wait-and-see solutions

This case is when the household loads and PV outputs are known before buying or selling energy in the DA market. A perfect information solution would choose optimal first-stage energy scheduling and procurement decisions for each realization of ξ. The expected value of this solution is known in the literature as the 'wait-and-see' (WS) solution, where:

$$WS = \mathbb{E}_{\xi}\left[\min_{x\in X} F(x,\xi)\right]$$

This case will achieve the minimum costs due to perfect information, though it is impossible to make perfect forecasts in practice.

2) Recourse problem (RP) solution

An alternative problem, *a stochastic program with fixed recourse* or the *recourse problem* (RP), is written as:

$$RP = \min_{x\in X} \mathbb{E}_{\xi}[F(x,\xi)]$$

In this case, possible realizations of uncertainty parameters are looped over, and balanced decisions with recourse are made. Note that when the uncertainty is revealed, additional or second stage actions can hedge the effect of uncertainty, so-called '*recourse actions*.'

3) Expected value solution

The expected value (EV) problem is an approximation of the RP problem, where:

$$EV = \min_{\mathbf{x}\in X} F(\mathbf{x},\bar{\xi})$$

This problem produces the first-stage solutions, $\bar{\mathbf{x}}(\bar{\xi})$, which become inventories to the second-stage optimization problem. The second-stage optimization must then be performed after ξ is realized.

$$Q(\bar{\boldsymbol{x}}(\bar{\xi}),\xi_s) = \min_{\boldsymbol{y}(\xi_s)} q(\boldsymbol{y}(\xi_s),\xi_s)$$
$$\text{subject to } \boldsymbol{g}_2(\bar{\boldsymbol{x}}(\bar{\xi}),\boldsymbol{y}(\xi_s),\xi_s) \leqslant 0, \boldsymbol{g}_2(\bar{\boldsymbol{x}}(\bar{\xi}),\boldsymbol{y}(\xi_s),\xi_s) = 0, \forall s \in S$$

In our context, the DA energy scheduling decisions are made based on the expectations of the forecasting results of sister forecasters. The house owner needs to import/export energy from/to the real-time retail market for balancing. The obtained day-ahead scheduling variables ($\bar{\mathbf{x}}[\bar{\xi}]$) are used in the second stage for balancing.

$$F(\bar{\boldsymbol{x}}(\bar{\xi}),\xi) = minf(\bar{\boldsymbol{x}}(\bar{\xi})) + y_{i,\xi}^{import}\cdot\mu_i^{buy} - y_{i,\xi}^{export}\cdot\mu_i^{sell}$$
$$\mathrm{y}_{i,\xi}^{RL} + \mathrm{y}_{i,\xi}^{BL} + \mathrm{y}_{i,\xi}^{CL} = L_{i,\xi}^{fix} + \bar{L}_i^{shift}$$
$$\mathrm{y}_{i,\xi}^{RL} + \mathrm{y}_{i,\xi}^{RB} + \mathrm{y}_{i,\xi}^{RC} = P_{i,\xi}^{PV}$$
$$P_{i,\xi}^{PV} + \bar{x}_i^{import} + y_{i,\xi}^{import} + y_{i,\xi}^{bat\_disch} = L_{i,\xi}^{fix} + \bar{L}_i^{shift} + \bar{x}_i^{export} + y_{i,\xi}^{export} + y_{i,\xi}^{bat\_ch}$$

The expected result of using the EV solution is then

$$EEV = \mathbb{E}_{\xi}[F(\bar{\mathbf{x}}(\bar{\xi}),\xi)]$$

4) The value of the stochastic solution

The following relations hold [29,48]:

$$WS \leq RP \leq EEV$$

$$EVPI = RP - WS$$

$$VSS = EEV - RP$$

The first relation $WS \leq RP$ states that it is always better to get the prior information of uncertainties. The second relation $RP \leq EEV$ envisions that it is always better to have recourse actions after the uncertainties are revealed than the results of simply averaging uncertainties. The difference between *RP* and *WS* is known as *EEPI* (>0), *the expected value of perfect information*. It is the maximal amount a decision-maker should spend to get the information in advance. The difference between *EEV* and *RP* is known as the *VSS* (>0), *the value of the stochastic solution*. It shows that dealing with uncertainties bring benefit than ignoring them.

Appendix C. The rule-based energy dispatch strategy

Rule-based PV-battery control (RBC) is straightforward and easy to implement in practice. In this study, a basic rule-based energy dispatch strategy is employed for benchmarking, and the flow chart of operation principle is depicted in Fig. 24.

The RBC approach in Fig. 24 utilizes priority-based energy dispatch strategies. When PV generation is higher than the demand, it will supply the

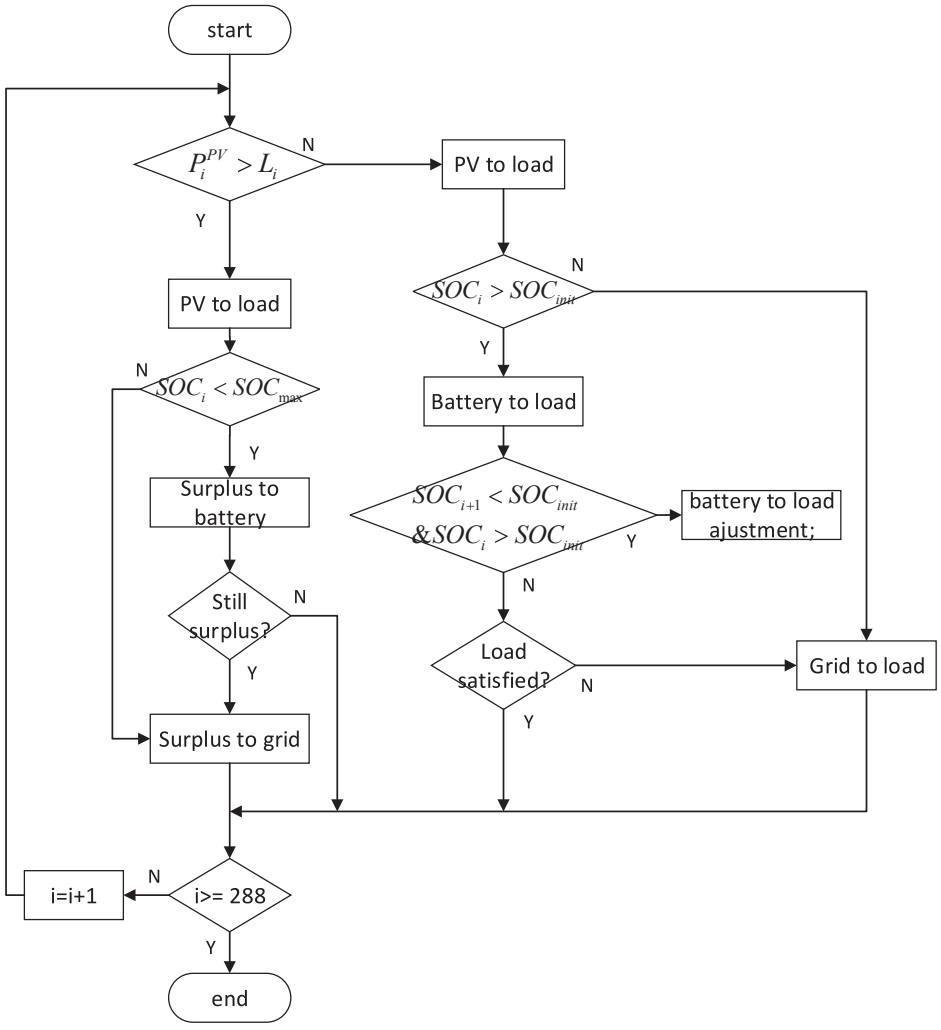

Fig. 24. Flow chart of the rule-based energy dispatch strategy.

demand first, and then the surplus PV energy is stored in the battery if it is not fully charged. If there is still surplus PV energy, the remains would be sold to the grid based on the feed-in tariff policy. When the PV generation cannot meet the load demand, the battery would discharge to support part of the load if there is available energy. Here, we only use battery for buffering surplus PV energy. Thus, we assume the battery can only discharge when there was surplus PV energy charged into the battery before ($SOC_i > SOC_{init}$). Otherwise, the household user will purchase electricity from the power grid. Note that we add a battery (dis-)charging power adjustment step by the condition of $SOC_{i+1} < SOC_{init} \& SOC_i > SOC_{init}$ to keep the SOC values within allowed ranges.

Fig. 25 shows the RBC energy scheduling results for the low PV installation home, and Fig. 26 shows the scheduling results for the high PV installation home using the same parameters and input data as the main content.

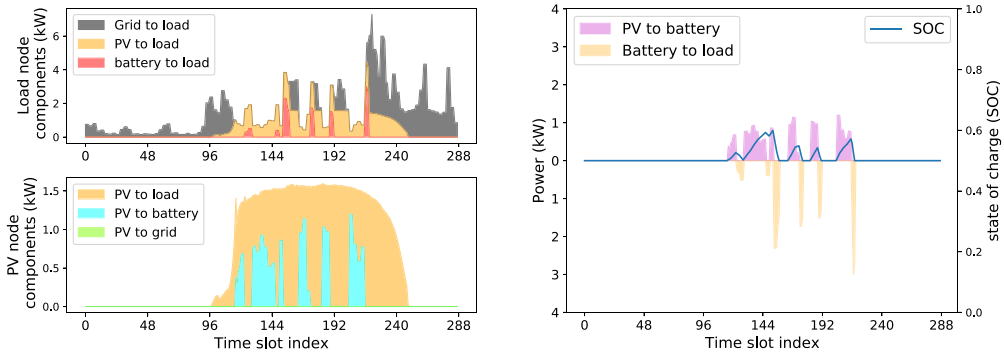

Fig. 25. Rule-based energy scheduling results of low PV-installation household ($cap^B = 10kWh, cap^{PV} = 10m^2$) (a) flowing-in and flowing-out components of Load and PV nodes, respectively, and (b) battery energy flows and its state of charge curve.

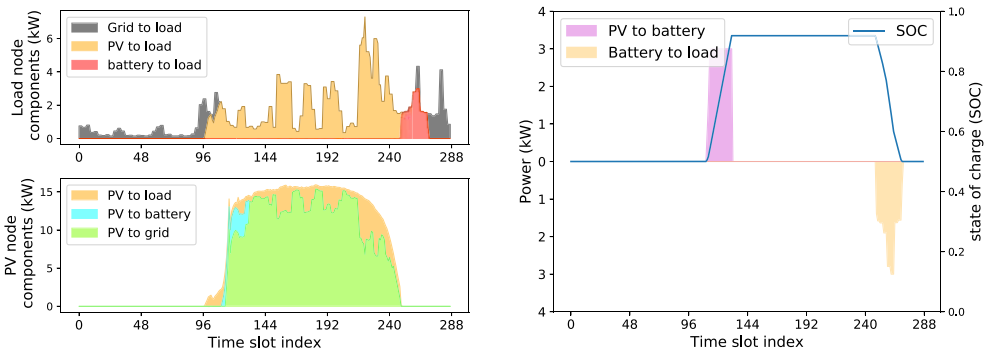

Fig. 26. Rule-based energy scheduling results of high PV-installation household ($cap^B = 10kWh, cap^{PV} = 100m^2$) (a) flowing-in and flowing-out components of Load and PV nodes, respectively, and (b) battery energy flows and its state of charge curve.

Appendix D. The hybrid control of RP and RBC methods

Fig. 27 shows the flow chart of the hybrid approach for battery (dis-)charging. The original battery (dis-)charging controls of the RP method is revised according to the rule that: 1) the surplus PV energy supplies the battery with higher priority than exporting to the RT market; 2) the original RT-imported electricity should be satisfied with battery discharging energy firstly. Similar to the RP and RBC approaches, the initial and ending battery SOCs are hold the same as 0.5 by readjusting in the final time slot.

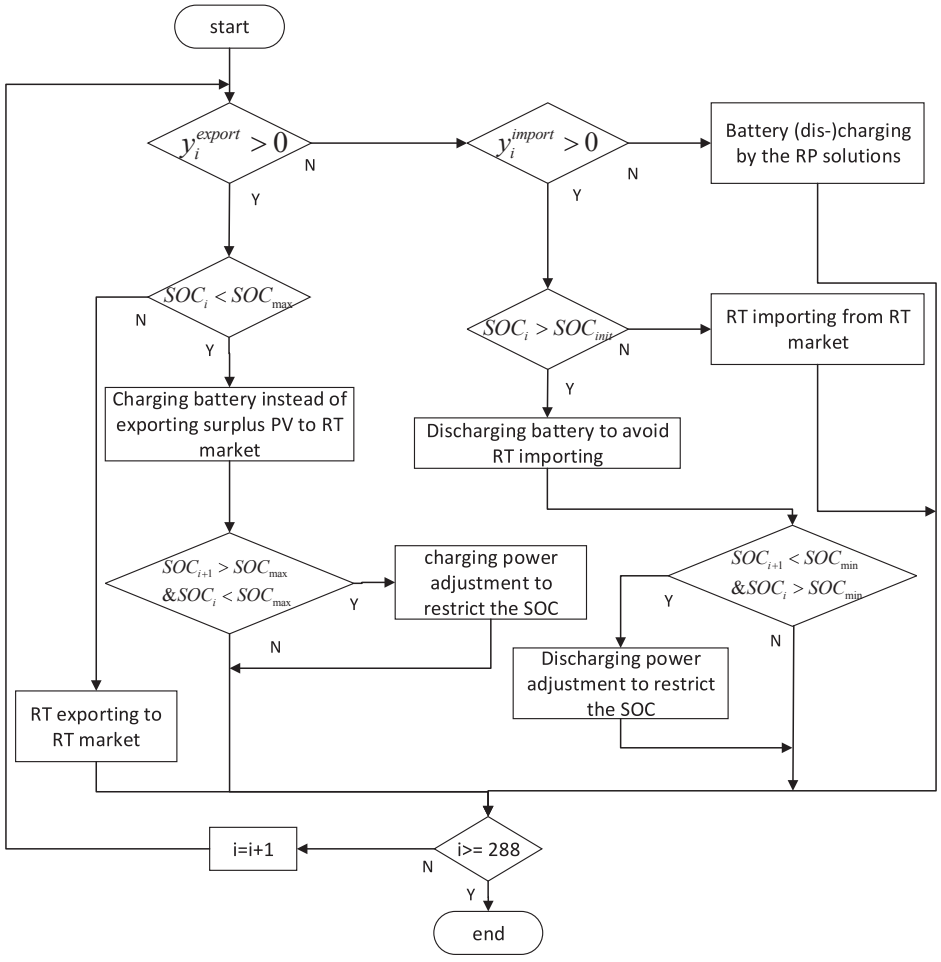

Fig. 27. Flow chart of the hybrid approach for the battery (dis-)charging control.

References

[1] HKEMSD. Hong Kong Energy End-use Data 2018. Https://WwwEmsdGovHk/Filemanager/En/Content_762/HKEEUD2018Pdf 2018.

[2] Department of Energy US. Quadrennial Technology Review: An Assessment ofEnergy Technologies and Research Opportunities 2015.

[3] Zhou B, Li W, Chan KW, Cao Y, Kuang Y, Liu X, et al. Smart home energy management systems: Concept, configurations, and scheduling strategies. Renew Sustain Energy Rev 2016;61:30–40. https://doi.org/10.1016/j.rser.2016.03.047.

[4] Yildiz B, Bilbao JI, Dore J, Sproul AB. Recent advances in the analysis of residential electricity consumption and applications of smart meter data. Appl Energy 2017;208:402–27. https://doi.org/10.1016/j.apenergy.2017.10.014.

[5] Abubakar I, Khalid SN, Mustafa MW, Shareef H, Mustapha M. Application of load monitoring in appliances' energy management – A review. Renew Sustain Energy Rev 2017;67:235–45. https://doi.org/10.1016/j.rser.2016.09.064.

[6] Hong T, Fan S. Probabilistic electric load forecasting: A tutorial review. Int J Forecast 2016;32:914–38. https://doi.org/10.1016/j.ijforecast.2015.11.011.

[7] Beaudin M, Zareipour H. Home energy management systems: A review of modelling and complexity. Renew Sustain Energy Rev 2015;45:318–35. https://doi.org/10.1016/j.rser.2015.01.046.

[8] Hu M, Xiao F, Wang S. Neighborhood-level coordination and negotiation techniques for managing demand-side flexibility in residential microgrids. Renew Sustain Energy Rev 2021;135:110248. https://doi.org/10.1016/j.rser.2020.110248.

[9] Yan J, Yang Y, Campana PE, He J. City-level analysis of subsidy-free solar photovoltaic electricity price, profits and grid parity in China. Nat Energy 2019;4. doi:10.1038/s41560-019-0441-z.

[10] BloombergNEF. Battery Pack Prices Cited Below $100/kWh for the First Time in 2020, While Market Average Sits at $137/kWh n.d. https://about.bnef.com/blog/battery-pack-prices-cited-below-100-kwh-for-the-first-time-in-2020-while-market-average-sits-at-137-kwh/ (Accessed: 12 April 2021).

[11] Zheng Z, Li X, Pan J, Luo X. A multi-year two-stage stochastic programming model for optimal design and operation of residential photovoltaic-battery systems. Energy Build 2021;239:110835. https://doi.org/10.1016/j.enbuild.2021.110835.

[12] Zheng Zhuang, Chen Hainan, Luo Xiaowei. A supervised event-based non-intrusive load monitoring for non-linear appliances. Sustainability 2018;10(4):1001. https://doi.org/10.3390/su10041001.

[13] Stephen B, Galloway S, Burt G. Self-learning load characteristic models for smart appliances. IEEE Trans Smart Grid 2014;5:2432–9. https://doi.org/10.1109/TSG.2014.2318375.

[14] Zhang X, Kato T, Matsuyama T. Learning a context-aware personal model of appliance usage patterns in smart home. 2014 IEEE Innov Smart Grid Technol - Asia, ISGT ASIA 2014 2014:73–8. doi:10.1109/ISGT-Asia.2014.6873767.

[15] Liang Z, Bian D, Zhang X, Shi D, Diao R, Wang Z. Optimal energy management for commercial buildings considering comprehensive comfort levels in a retail electricity market. Appl Energy 2019;236:916–26. https://doi.org/10.1016/j.apenergy.2018.12.048.

[16] Pamulapati T, Mallipeddi R, Lee M. Multi-objective home appliance scheduling with implicit and interactive user satisfaction modelling. Appl Energy 2020;267:114690. https://doi.org/10.1016/j.apenergy.2020.114690.

[17] Rocha HRO, Honorato IH, Fiorotti R, Celeste WC, Silvestre LJ, Silva JAL. An Artificial Intelligence based scheduling algorithm for demand-side energy management in Smart Homes. Appl Energy 2021;282:116145. https://doi.org/10.1016/j.apenergy.2020.116145.

[18] Amara F, Agbossou K, Dubé Y, Kelouwani S, Cardenas A, Bouchard J. Household electricity demand forecasting using adaptive conditional density estimation. Energy Build 2017;156:271–80. https://doi.org/10.1016/j.enbuild.2017.09.082.

[19] Amara F, Agbossou K, Dubé Y, Kelouwani S, Cardenas A, Hosseini SS. A residual load modeling approach for household short-term load forecasting application. Energy Build 2019;187:132–43. https://doi.org/10.1016/j.enbuild.2019.01.009.

[20] Hong T, Pinson P, Fan S, Zareipour H, Troccoli A, Hyndman RJ. Probabilistic energy forecasting: global energy forecasting competition 2014 and beyond. Int J Forecast 2016;32:896–913. https://doi.org/10.1016/j.ijforecast.2016.02.001.

[21] Hobby JD, Shoshitaishvili A, Tucci GH. Analysis and methodology to segregate residential electricity consumption in different taxonomies. IEEE Trans Smart Grid 2012;3:217–24. https://doi.org/10.1109/TSG.2011.2167353.

[22] Zheng Z, Chen H, Luo X. A Kalman fi lter-based bottom-up approach for household short-term load forecast. Appl Energy 2019;250:882–94. https://doi.org/10.1016/j.apenergy.2019.05.102.

[23] Wang Y, Gan D, Sun M, Zhang N, Lu Z, Kang C. Probabilistic individual load forecasting using pinball loss guided LSTM. Appl Energy 2019;235:10–20. https://doi.org/10.1016/j.apenergy.2018.10.078.

[24] Zhang S, Wang Y, Zhang Y, Wang D, Zhang N. Load probability density forecasting by transforming and combining quantile forecasts. Appl Energy 2020;277:115600. https://doi.org/10.1016/j.apenergy.2020.115600.

[25] Hosseini SS, Agbossou K, Kelouwani S, Cardenas A. Non-intrusive load monitoring through home energy management systems: A comprehensive review. Renew Sustain Energy Rev 2017;79:1266–74. https://doi.org/10.1016/j.rser.2017.05.096.

[26] Lusis P, Rajab K, Andrew L, Liebman A. Short-term residential load forecasting : Impact of calendar e ff ects and forecast granularity 2017;205:654–69. doi:10.1016/j.apenergy.2017.07.114.

[27] Hosseini SM, Carli R, Dotoli M. Robust Optimal Energy Management of a Residential Microgrid Under Uncertainties on Demand and Renewable Power Generation. IEEE Trans Autom Sci Eng 2020;18(2). https://doi.org/10.1109/TASE.2020.2986269.

[28] Shi R, Li S, Zhang P, Lee KY. Integration of renewable energy sources and electric vehicles in V2G network with adjustable robust optimization. Renew Energy 2020;153:1067–80. https://doi.org/10.1016/j.renene.2020.02.027.

[29] Birge JR, Louveaux F. Introduction to stochastic programming. 2011. doi:10.1007/0-387-33477-7.

[30] Correa-Florez CA, Gerossier A, Michiorri A, Kariniotakis G. Stochastic operation of home energy management systems including battery cycling. Appl Energy 2018;225:1205–18. https://doi.org/10.1016/j.apenergy.2018.04.130.

[31] Sousa T, Soares T, Pinson P, Moret F, Baroche T, Sorin E. Peer-to-peer and community-based markets: a comprehensive review. Renew Sustain Energy Rev 2018;104:367–78. https://doi.org/10.1016/j.rser.2019.01.036.

[32] Wang Z, Yu X, Mu Y, Jia H. A distributed Peer-to-Peer energy transaction method for diversified prosumers in Urban Community Microgrid System. Appl Energy 2020;260:114327. https://doi.org/10.1016/j.apenergy.2019.114327.

[33] Moret F, Pinson P. Energy collectives: a community and fairness based approach to future electricity markets. IEEE Trans Power Syst 2019;34:3994–4004. https://doi.org/10.1109/TPWRS.2018.2808961.

[34] Jeddi B, Mishra Y, Ledwich G. Distributed Load Scheduling in Residential Neighborhoods for Coordinated Operation of Multiple Home Energy Management Systems. ArXiv E-Prints n.d.

[35] Carli R, Dotoli M. Decentralized control for residential energy management of a smart users ' microgrid with renewable energy exchange. IEEE/CAA J Autom Sin 2019;6. https://doi.org/10.1109/JAS.2019.1911462.

[36] Paudel A, Chaudhari K, Long C, Gooi HB. Peer-to-peer energy trading in a prosumer-based community microgrid: A game-theoretic model. IEEE Trans Ind Electron 2019;66:6087–97. https://doi.org/10.1109/TIE.2018.2874578.

[37] Mohsenian-Rad AH, Wong VWS, Jatskevich J, Schober R. Optimal and autonomous incentive-based energy consumption scheduling algorithm for smart grid. Innov Smart Grid Technol Conf ISGT 2010;2010:1–6. https://doi.org/10.1109/ISGT.2010.5434752.

[38] Scarabaggio P, Member GS, Grammatico S, Member S, Carli R, Dotoli M, et al. Distributed demand side management with stochastic wind power forecasting. IEEE Trans Control Syst Technol 2021:1–16. https://doi.org/10.1109/TCST.2021.3056751.

[39] Liu N, Yu X, Wang C, Li C, Ma L, Lei J. Energy-sharing model with price-based demand response for microgrids of peer-to-peer prosumers. IEEE Trans Power Syst 2017;32:3569–83. https://doi.org/10.1109/TPWRS.2017.2649558.

[40] Yang P, Chavali P, Gilboa E, Nehorai A. Parallel load schedule optimization with renewable distributed generators in smart grids. IEEE Trans Smart Grid 2013;4:1431–41. https://doi.org/10.1109/TSG.2013.2264728.

[41] Chavali P, Yang P, Nehorai A. A distributed algorithm of appliance scheduling for home energy management system. IEEE Trans Smart Grid 2014;5:282–90. https://doi.org/10.1109/TSG.2013.2291003.

[42] Zhou Y, Wu J, Long C. Evaluation of peer-to-peer energy sharing mechanisms based on a multiagent simulation framework. Appl Energy 2018;222:993–1022. https://doi.org/10.1016/j.apenergy.2018.02.089.

[43] Bokde N, Asencio-Cortés G, Martínez-álvarez F, Kulat K. PSF: Introduction to R package for pattern sequence based forecasting algorithm. R J 2017;9:324–33. https://doi.org/10.32614/rj-2017-021.

[44] Mhanna S, Chapman AC, Verbic G. A fast distributed algorithm for large-scale demand response aggregation. IEEE Trans Smart Grid 2016;7:2094–107. https://doi.org/10.1109/TSG.2016.2536740.

[45] IEEE Open Data Set - Consumption n.d. https://site.ieee.org/pes-iss/data-sets/ (Accessed: 12 January 2021).

[46] IEEE Open Data Set - PV Generation n.d. https://site.ieee.org/pes-iss/data-sets/ (Accessed: 12 January 2021).

[47] Barker S, Mishra A, Irwin D, Cecchet E, Shenoy P, Albrecht J. Smart*: An Open Data Set and Tools for Enabling Research in Sustainable Homes. SustKDD 2012:6.

[48] Birge JR. The value of the stochastic solution in stochastic linear programs with fixed recourse. Math Program 1982;24:314–25. https://doi.org/10.1007/BF01585113.

[49] Bertsekas DP, Tsitsiklis JN. Parallel and distributed computation: numerical methods-introduction. Englewood Cliffs 1989:1–94. https://doi.org/10.1016/b978-0-12-093480-5.50005-2.